

This is an Open Access document downloaded from ORCA, Cardiff University's institutional repository: <https://orca.cardiff.ac.uk/id/eprint/165357/>

This is the author's version of a work that was submitted to / accepted for publication.

Citation for final published version:

Samer, Carolyn, McWilliam, Hamish E.G., McSharry, Brian P., Velusamy, Thilaga, Burchfield, James G., Stanton, Richard J., Tscharke, David C., Rossjohn, Jamie, Villadangos, Jose A., Abendroth, Allison and Slobedman, Barry 2024. Multi-targeted loss of the antigen presentation molecule MR1 during HSV-1 and HSV-2 infection. *iScience*, 108801. 10.1016/j.isci.2024.108801

Publishers page: <http://dx.doi.org/10.1016/j.isci.2024.108801>

Please note:

Changes made as a result of publishing processes such as copy-editing, formatting and page numbers may not be reflected in this version. For the definitive version of this publication, please refer to the published source. You are advised to consult the publisher's version if you wish to cite this paper.

This version is being made available in accordance with publisher policies. See <http://orca.cf.ac.uk/policies.html> for usage policies. Copyright and moral rights for publications made available in ORCA are retained by the copyright holders.



Journal Pre-proof



Multi-targeted loss of the antigen presentation molecule MR1 during HSV-1 and HSV-2 infection

Carolyn Samer, Hamish E.G. McWilliam, Brian P. McSharry, Thilaga Velusamy, James G. Burchfield, Richard J. Stanton, David C. Tschärke, Jamie Rossjohn, Jose A. Villadangos, Allison Abendroth, Barry Slobedman

PII: S2589-0042(24)00022-1

DOI: <https://doi.org/10.1016/j.isci.2024.108801>

Reference: ISCI 108801

To appear in: *ISCIENCE*

Received Date: 16 March 2023

Revised Date: 18 September 2023

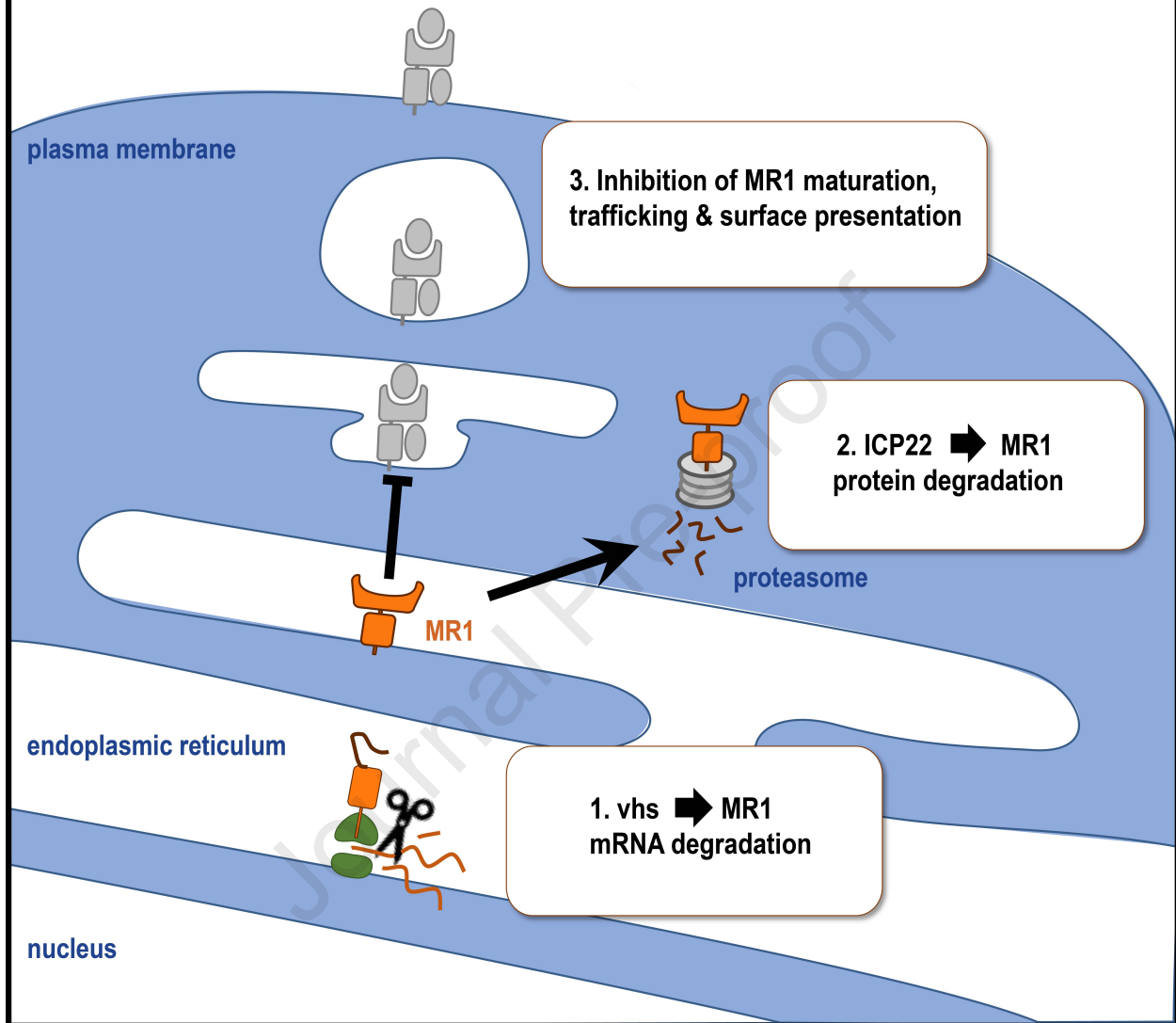
Accepted Date: 2 January 2024

Please cite this article as: Samer, C., McWilliam, H.E.G., McSharry, B.P., Velusamy, T., Burchfield, J.G., Stanton, R.J., Tschärke, D.C., Rossjohn, J., Villadangos, J.A., Abendroth, A., Slobedman, B., Multi-targeted loss of the antigen presentation molecule MR1 during HSV-1 and HSV-2 infection, *ISCIENCE* (2024), doi: <https://doi.org/10.1016/j.isci.2024.108801>.

This is a PDF file of an article that has undergone enhancements after acceptance, such as the addition of a cover page and metadata, and formatting for readability, but it is not yet the definitive version of record. This version will undergo additional copyediting, typesetting and review before it is published in its final form, but we are providing this version to give early visibility of the article. Please note that, during the production process, errors may be discovered which could affect the content, and all legal disclaimers that apply to the journal pertain.

© 2024

Herpes simplex virus proteins vhs and ICP22 inhibit MR1 antigen presentation



1 **Multi-targeted loss of the antigen presentation molecule** 2 **MR1 during HSV-1 and HSV-2 infection**

3
4 Carolyn Samer¹, Hamish E. G. McWilliam^{2,3}, Brian P. McSharry^{1,4}, Thilaga Velusamy⁵, James G.
5 Burchfield^{6,7}, Richard J. Stanton⁸, David C. Tschärke⁵, Jamie Rossjohn^{8,9}, Jose A. Villadangos^{2,3}, Allison
6 Abendroth^{1#}, Barry Slobedman^{1#*}

7
8 ¹Infection, Immunity and Inflammation, School of Medical Sciences, Faculty of Medicine and Health,
9 and the Charles Perkins Centre, The University of Sydney, NSW, Australia.

10 ²Department of Microbiology and Immunology, Peter Doherty Institute for Infection and Immunity,
11 The University of Melbourne, Melbourne, VIC, Australia.

12 ³Department of Biochemistry and Pharmacology, Bio21 Molecular Science and Biotechnology
13 Institute, The University of Melbourne, Parkville, VIC, Australia.

14 ⁴School of Dentistry and Medical Sciences, Faculty of Science and Health, Charles Sturt University,
15 Wagga Wagga, NSW, Australia.

16 ⁵John Curtin School of Medical Research, Australian National University, Canberra, Australian Capital
17 Territory, Australia.

18 ⁶Charles Perkins Centre, The University of Sydney, Sydney, NSW, Australia.

19 ⁷School of Life and Environmental Sciences, University of Sydney, Sydney, NSW, Australia.

20 ⁸Division of Infection & Immunity, School of Medicine, Cardiff University, Cardiff, Wales.

21 ⁹Infection and Immunity Program, Department of Biochemistry and Molecular Biology, Biomedicine
22 Discovery Institute, Monash University, VIC, Australia.

23
24 # Equal contribution

25
26 * Lead contact: Barry Slobedman

27 Correspondence: barry.slobedman@sydney.edu.au

28 **Summary**

29 The Major Histocompatibility Complex (MHC), Class-I-related (MR1) molecule presents microbiome-
30 synthesised metabolites to Mucosal-associated invariant T (MAIT) cells, present at sites of herpes
31 simplex virus (HSV) infection. During HSV type 1 (HSV-1) infection there is a profound and rapid loss
32 of MR1, in part due to expression of unique short (US)3 protein. Here we show that virion host shutoff
33 (vhs) RNase protein downregulates MR1 protein, through loss of MR1 transcripts. Furthermore, a third
34 viral protein, infected cell protein (ICP)22, also downregulates MR1, but not classical MHC-I molecules.
35 This occurs early in the MR1 trafficking pathway through proteasomal degradation. Finally, HSV-2
36 infection results in the loss of MR1 transcripts, and intracellular and surface MR1 protein, comparable
37 to that seen during HSV-1 infection. Thus HSV coordinates a multifaceted attack on the MR1 antigen
38 presentation pathway, potentially protecting infected cells from MAIT cell TCR-mediated detection at
39 sites of primary infection and reactivation.

40

41

42 Introduction

43 Mucosal-associated invariant T (MAIT) cells are a tissue resident and circulating memory T cell
44 population that play key roles monitoring and responding to changes in the integrity of mucosal and
45 barrier sites.¹⁻⁴ MAIT cells are pleiotropic innate-like T cells due to their expression of multiple
46 transcription factors including PLZF,⁵ their restricted repertoire of T cell receptors (TCR) and activation
47 through TCR dependent and independent mechanisms.⁶⁻¹⁰ Through TCR binding, MAIT cells recognise
48 bacterial or fungal-sourced intermediates from the vitamin B biosynthesis pathway presented by the
49 Major Histocompatibility Complex, Class-I-related (MR1) molecule.¹¹ This allows MAIT cells to detect
50 specific perturbations in the metabolome resulting from changes in the composition or location of the
51 microbiome and pathogens.

52 Unlike classical T cells, MAIT cells can be activated by cytokines and Toll like receptor (TLR) agonists
53 that can also arise from diverse viral infections. Indeed, there is a growing appreciation of the
54 importance of MAIT cell protection against viral infections including influenza A virus,⁹ Hepatitis C¹²
55 and HIV-1.¹³ MAIT cells are more abundant in the blood during dengue virus, correlating with disease
56 severity,¹² while during early HIV infection blood and mucosal MAIT cells are activated and expanded,
57 potentially responding to increased microbial translocation.¹⁴ However in many viral infections
58 including human T lymphotropic virus type 1,¹⁵ Influenza A virus,^{10,12} Hepatitis B virus,¹⁶⁻¹⁹ Hepatitis C
59 virus,^{12,20,21} Hepatitis D virus,¹⁸ chronic HIV²²⁻²⁵ and SARS-CoV-2,^{26,27} circulating and tissue resident
60 MAIT cells are reduced in number, often expressing an exhausted phenotype.

61 MAIT TCR-mediated signalling in the absence of other markers of infection drives a Th17 tissue repair
62 phenotype.^{28,29} Although MAIT cells express a pro-inflammatory Th1 signature in response to TCR
63 independent factors, sustained activation with concurrent proliferation and targeted cytotoxicity
64 requires the addition of TCR signalling.^{1,30-32} While there is no evidence that viruses synthesise MR1
65 ligands, it is clear that viruses such as the human herpesviruses, modulate the MR1-TCR MAIT cell
66 axis.³³ Recent studies have also confirmed that riboflavin availability enhances MAIT cell protective
67 responses to influenza A virus infections in mice,³⁴ and inhibits entry of flaviviruses.³⁵ Herpesviruses
68 establish a primary infection in the skin, lungs, orofacial and genital mucosa, at sites colonised by MR1
69 ligand producing bacteria and monitored by immune cell populations including MAIT cells. During
70 primary lytic infection, virally-induced disruptions at these barrier sites could increase MR1 antigen
71 availability, driving the early activation arm of resident MAIT cells, with consequent TCR-mediated
72 cytolysis of virally-infected host cells. The synergistic MAIT cell activation associated with antiviral
73 cytokines combined with this TCR signal, would enhance the proinflammatory response of MAIT cells;
74 a result that could strongly impact viral replication and transmission efficiency. Furthermore, a subset

75 of MAIT cells respond to surface MR1 in the absence of microbial ligands, promoting T-helper like
76 functionality, including DC maturation.³⁶ In all these scenarios, disabling the MR1-TCR response would
77 represent an advantage to viral survival.

78 We previously reported that herpes simplex virus type 1 (HSV-1), human cytomegalovirus (HCMV) and
79 varicella zoster virus (VZV) all downregulate MR1 expression.³⁷⁻³⁹ During HSV-1 infection, substantial
80 loss of MR1 protein is detected during early infection, predominantly from the immature protein
81 accumulating in the endoplasmic reticulum (ER) awaiting exogenous ligand.³⁷ Although pre-existing
82 surface MR1 remains protected from HSV-1 induced loss, there is a substantial reduction in new
83 surface MR1 resulting from depletion of the ER pool. While the viral kinase unique short (US)3 and
84 homolog open reading frame (ORF)66 are implicated in MR1 inhibition in HSV-1 and VZV infections
85 respectively, viruses lacking their expression fail to fully rescue the loss,^{37,38} suggesting that additional
86 viral products contribute to this suppression of MR1 expression.

87 HSV encodes approximately 84 viral gene products, which are expressed in a three-step immediate-
88 early (IE), early (E), and late (L) sequential cascade.⁴⁰ IE products, which are synthesised immediately
89 post release of the viral DNA into the host's nucleus, inhibit critical antiviral functions and promote
90 pro-viral gene transcription and protein synthesis.⁴¹⁻⁴³ Here we provide evidence that one of these
91 products, namely ICP22, contributes to the loss of ER-resident MR1 through proteasomal degradation.
92 In contrast, a second IE protein, ICP47, which blocks peptide presentation by MHC-I molecules to
93 classical T cells, does not play an apparent role in MR1 modulation. In addition, an HSV-1 late
94 expressed protein, the virion host shutoff (vhs) RNase protein encoded by the unique long (UL)41
95 gene, contributes to the loss of MR1 protein through the downregulation of MR1 transcripts. We also
96 report that a third alphaherpesvirus, HSV-2, modulates MR1 protein, replicating the HSV-1 mediated
97 loss of immature MR1 and ligand-dependent modulation of antigen-bound surface molecules.
98 Together these results expand the number of viruses that modulate this non-classical antigen
99 presentation molecule and reveal that HSV-1 encodes multiple mechanisms to produce this
100 immunomodulatory effect.

101

102 Results

103 TAP inhibitor ICP47 modulates MHC-I but not MR1 antigen presentation

104 Loss of cellular MR1 is detectable within four hours of HSV-1 infection in epithelial cells,³⁷ implicating
105 one of the five IE proteins expressed immediately post viral entry. We have previously established
106 that the IE E3 ubiquitin ligase protein ICP0 is not responsible for the loss of MR1 protein during HSV-
107 1 infection.³⁷ A second IE protein, ICP47, is well characterised for its ability to inhibit classical MHC-I
108 antigen presentation. ICP47 inhibits the transporter associated with antigen processing (TAP) protein
109 dimer, thus preventing the delivery of peptides across the ER membrane into the lumen for loading
110 into the MHC-I antigenic cleft.^{41,44,45} TAP is part of the peptide loading complex (PLC) which can
111 stabilise two antigen presentation molecules simultaneously.⁴⁶ Components of the PLC contribute to
112 MR1 stability and antigen loading in the ER,⁴⁷ consequently viral interference may indirectly impact
113 MR1 stability.

114 To test whether expression of ICP47 during infection impacts MR1 antigen presentation, ARPE-19
115 epithelial cells were infected with HSV-1 KOS strain and ICP47 null mutant ICP47del⁴⁸ and analysed by
116 flow cytometry. Equivalent surface expression of the late viral glycoprotein gC was detected at 6 h
117 post infection (p.i.) in the cells infected with both parental and mutant viruses (Fig. 1.A) confirming
118 that deletion of the non-essential ICP47 protein had no impact on expression kinetics at this early
119 timepoint. As expected, compared to mock infected cells, surface MHC-I expression was
120 downregulated by the parental virus, but not the mutant virus (Fig. 1.B), recapitulating the role ICP47
121 plays in the early loss of surface MHC-I.^{49,50}

122 Increased surface MR1 associated with Ac-6-FP ligand-induced maturation and plasma membrane
123 trafficking can be detected after 2 hours, and peaks around 8 hours post treatment.⁵¹ In order to
124 examine the effect of an IE viral gene on both total cellular MR1 and surface MR1, ARPE-19 cells
125 transduced to express MR1-GFP³⁷ were treated with Ac-6-FP ligand 3 h p.i., after substantial IE gene
126 expression,⁵² and then harvested 3 hours later. Both viruses invoked a similar loss of total MR1 as
127 detected by the GFP signal (Fig. 1.C) however, consistent with previous reports, no loss of surface MR1
128 was evident at this early timepoint.³⁷ In cells similarly infected but treated with ligand 4 hours prior to
129 staining at 18 h p.i., a timepoint associated with complete gene expression and high yield of viral
130 progeny,⁵³ the strong loss of both total and surface MR1 was again comparable in the parental and
131 mutant infected cells (Fig. 1.D). Given the lack of rescue of total or surface MR1 by ICP47del at both
132 early and late timepoints, this suggests that inhibition of TAP functionality by ICP47 does not interfere

133 with PLC-mediated stability of MR1 in the ER, and consequently does not contribute to the loss of MR1
134 during HSV-1 infection.

135 **ICP22 viral protein promotes proteasomal degradation of MR1**

136 The three remaining IE proteins, ICP4, ICP22 and ICP27, use multiple mechanisms to initiate and
137 promote viral gene expression, at the expense of cellular expression, through interactions with
138 cellular transcription and translation machinery. ICP22 is broadly characterised as a pro-viral trans
139 regulator, without which viral replication is severely attenuated and viral progeny contain reduced
140 amounts of some glycoproteins.⁵⁴ ICP22 is attributed with diverse roles during HSV-1 replication
141 including the recruitment of cellular chaperones into nuclear virus enriched chaperone enhanced
142 (VICE) domains adjacent to the viral replication centres,⁵⁵⁻⁵⁷ modulation of RNA polymerase (pol) II⁵⁸⁻
143 ⁶¹ and modulation of cell cycling.^{62,63} Of particular interest, ICP22 may act as a J-protein co-chaperone,
144 interacting with cellular Hsc70 protein to manage misfolded proteins.⁵⁷ In addition, HSV-2 ICP22 E3
145 ubiquitin ligase functionality is responsible for ubiquitination, and subsequent degradation, of several
146 signal transducer proteins in the type 1 interferon signalling pathway.⁶⁴ Consequently, ICP22 qualified
147 as an interesting candidate for MR1 modulation.

148 To assess the impact of ICP22 expression on endogenous MR1 surface expression, the US1 gene from
149 HSV-1 strain F was cloned into the pCDH_EF1-MCS-T2A-copGFP plasmid (pSY10) upstream of a T2A
150 ribosomal skip sequence, thus facilitating the independent translation of GFP from the same transcript
151 as a marker of successful transfection. 293T cells transfected with either parental (pSY10) or the US1
152 expressing (pSY10-ICP22) plasmid were treated with Ac-6-FP ligand 6 hours prior to harvesting at 28
153 h p.i., at which point GFP was detectable in a subset of cells. The fold change in surface MHC-I and MR1
154 was calculated in GFP⁺ cells compared to non-transfected GFP⁻ cells within the same sample. No
155 difference in surface MR1 or MHC-I was associated with transfection of the parental plasmid
156 compared to mock-infected cells (Fig. 2.A). Expression of ICP22 however resulted in a marked
157 reduction in surface MR1 expression. By contrast MHC-I was instead upregulated in the ICP22-
158 expressing cells suggesting a differential effect of ICP22 on these related antigen presenting
159 molecules.

160 A second protein, US1.5, is translated from the US1 gene, however there is uncertainty regarding
161 which of the in frame start codons initiates the carboxyl-terminant molecule.^{58,65,66} During viral
162 infection both ICP22 and US1.5 are expressed; though the latter only accumulates at later timepoints
163 under the control of the US3 and UL13 viral kinases.⁶⁶

164 Both HSV-1 strain F ICP22 and US1.5 from codon 171^{60,66} were cloned with an N-terminal FLAG tag⁵⁸
165 into the replication incompetent pAdZ5-C5 adenovirus vector.⁶⁷ ARPE-19 MR1-GFP cells were infected
166 with parental (RAd-Ctrl), ICP22 (RAd-ICP22) or US1.5 (RAd-US1.5) expressing virus, at an MOI of 100,
167 for detection of total cellular MR1 and surface MR1 and MHC-I by flow cytometry. Cells were
168 optionally treated with Ac-6-FP ligand 4 hours (Post) prior to harvesting at 44 h p.i. At this timepoint
169 mild adenovirus-associated cytopathic effect was detected, reflecting successful adenovirus infection,
170 however there was minimal cell death associated with overexpression of the viral genes, that was
171 evident at later timepoints. In parallel, ARPE-19 cells expressing MR1 were similarly infected and
172 harvested to detect the size of the expressed protein through FLAG probe by immunoblot (Fig. 2.C).
173 Compared to mock-infected cells, adenovirus infection resulted in a small but significant increase in
174 total but not surface MR1, in an MOI-dependent manner. As a consequence, all statistical analysis of
175 the modulation of MR1-GFP, surface MR1 and MHC-I by viral genes was calculated relative to the
176 parental virus, with matching MOI, rather than mock-infected cells. Compared to cells infected with
177 RAd-Ctrl (Fig. 2.B, dotted line) both ICP22 and US1.5 expression reduced total cellular MR1-GFP levels
178 regardless of ligand treatment, although the reduction induced by US1.5 was significantly less than
179 that induced by the full length protein. The loss of cellular MR1 but not MHC-I was reconfirmed in the
180 adenovirus infected ARPE-19 MR1 cells which were lysed at 44 h p.i. and probed for MR1 and HLA-
181 ABC by western blot (Fig. 2.C).

182 Reductions in surface MR1 replicated that of cellular MR1 suggesting that depleted levels of
183 intracellular MR1 may be responsible for the loss of surface expression. Interestingly, although
184 transfection of 293T cells with the ICP22 expressing plasmid resulted in increased surface MHC-I (Fig.
185 2.A), there was no significant difference in surface expression resulting from either ICP22 or US1.5 via
186 adenovirus expression, nor was there any reduction in protein detected by western blot (Fig. 2.C).

187 Given that HSV-1 ICP22 downregulated expression of MR1 from both endogenous and foreign (murine
188 stem cell virus LTR) promoters, but did not similarly affect endogenously expressed MHC-I, it was
189 hypothesised that the viral genes specifically impacted MR1 protein rather than any MR1-specific or
190 global impact on transcripts. Although MR1 antigen presentation is proteasome-independent,⁶⁸ the
191 substantial portion of MR1 that accumulates in the ER is likely degraded through proteasomal ER-
192 associated degradation pathways.⁵¹ We previously reported that HSV-1 targets immature MR1 for
193 proteasomal degradation, by some unknown viral agent.³⁷ Indeed, treating the adenovirus infected
194 ARPE-19 MR1-GFP cells for 16 hours with proteasomal inhibitor MG132 (5 μ M) demonstrated a
195 significant rescue of MR1-GFP compared to vehicle control (Fig. 2.D), that was not explained by any

196 reduction in ICP22 or US1.5 protein expression (Fig. 2.E). This was rescue was not observed with
197 lysosomal inhibitor folimycin (50 nM).

198 Together this data demonstrates HSV-1 viral ICP22 (US1), and to a lesser extent the short form US1.5,
199 promote proteasomal degradation of MR1, impacting its ability to respond to ligand availability and
200 traffic to the plasma membrane. This downregulation is specific to MR1 and not applicable to classical
201 antigen presentation MHC-I molecules.

202 **vhs contributes to the loss of cellular MR1**

203 Although ectopic ICP22 and US1.5 expression resulted in a significant loss of MR1-GFP it is possible
204 that other viral proteins contribute to the profound downregulation of cellular MR1 evident during
205 HSV-1 infection.³⁷ The HSV-1 UL41 gene encodes a viral mRNA-specific endoribonuclease called virion
206 host shutoff protein (vhs), that degrades predominantly cellular transcripts⁶⁹⁻⁷¹ through association
207 with members of the cap binding complex including the RNA helicase accessory factor eIF4H.^{72,73}
208 Inhibition of cellular protein synthesis occurs immediately post infection with the release of vhs from
209 infecting viral particles, followed by a second stronger wave of transcript degradation with the *de novo*
210 expression of the late expression UL41 gene.⁵²

211 To evaluate the impact of vhs expression on MR1, HSV-1 strain F UL41 gene was cloned into the pAdZ5-
212 C5 adenovirus vector (RAd-vhs) and ARPE-19 MR1-GFP cells were infected as described. As detected
213 by flow cytometry, cellular MR1 was strongly downregulated by 44 h p.i. regardless of ligand
214 treatment (Fig. 3.A). Surface MR1 was also suppressed, with ligand treatment failing to promote
215 strong surface expression, presumably due to the substantial depletion of cellular MR1. By contrast,
216 endogenous surface MHC-I was only weakly downregulated by vhs expression. MR1 was not
217 detectable by western blot from RAd-vhs infected ARPE-19 MR1 cells at 44 h p.i. (Fig. 3.B). Despite the
218 modest loss of surface MHC-I detected by flow cytometry (Fig. 3.A) a strong loss of cellular MHC-I
219 proteins was evident (Fig. 3.B).

220 **MR1 transcripts are downregulated during HSV-1 infection**

221 Through alternative splicing the MR1 gene encodes four different protein isoforms.⁷⁴ The dominant
222 and best characterised isoform encoded by the MR1A splice variant is responsible for activation of
223 MAIT cells. The shorter MR1B protein lacks the α 3 extracellular domain and accumulates in the ER as
224 a homodimer rather than binding to β 2m.⁷⁵ There is conflicting evidence as to whether MR1B traffics
225 to the plasma membrane to activate MAIT cells or whether it plays a regulatory role by binding and
226 retaining antigen in the ER.^{75,76} The function of a soluble form lacking the transmembrane domain

227 (MR1C) and another lacking the $\alpha 3$ domain but encoding a long 3' untranslated sequence (MR1D)
228 remain completely uncharacterised. Given that ectopic expression of vhs resulted in a strong
229 downregulation of over-expressed MR1 protein, the relative amount of endogenous and over-
230 expressed transcripts were examined in human fibroblasts (HF) and ARPE-19 MR1 cells infected with
231 HSV-1 strain F at 2, 6 and 16 h p.i. Primers complementary to $\alpha 1$ and $\alpha 2$ regions were employed to
232 detect total transcripts for MR1A, MR1B and MR1C isoforms (MR1). Total MR1 transcripts were
233 significantly reduced in infected HF cells by 6 h p.i. with further loss at the later timepoint (Fig. 4.A).
234 In the ARPE-19 MR1 cells, where endogenous MR1 transcripts are likely outnumbered by the over
235 expressed MR1A isoform, this loss was detected at the 2 hour timepoint and further reduced as the
236 infection progressed (Fig. 4.B).

237 While vhs plays a key role in modulation of the host transcriptome, other viral proteins contribute to
238 this phenotype including ICP4, ICP27 and ICP22.^{77,78} To determine whether virus lacking vhs expression
239 rescued the loss of MR1 transcripts, HF cells were infected for 6 hours with HSV-1 17syn⁺ strain or the
240 corresponding vhs deletion mutant 17(41-).⁷⁹ Two additional primers positioned at splice sites to
241 specifically detect the MR1A and MR1B isoforms⁷⁶ were used to evaluate whether one isoform was
242 preferentially targeted. There was a significant downregulation of the MR1A isoform and the
243 combined isoforms from the intact parental virus, and although there was a similar loss of MR1B, it
244 was not statistically significant ($p=0.0753$) (Fig. 4.C). Infection with the vhs mutant virus resulted in
245 recovery of MR1A, MR1B and total MR1 transcripts, with no significant difference to mock-infected
246 cells. Again, although the trend was evident, the difference in MR1A isoforms between the parent and
247 mutant virus was not statistically significant.

248 **HSV-1 vhs mutant partially recovers loss of total MR1-GFP during early** 249 **infection**

250 At a late timepoint of infection the HSV-1 vhs deletion mutant does not rescue the loss of MR1,³⁷
251 however here we show that the vhs-mediated loss of MR1 transcripts is rescued at early timepoints
252 with the 17(41-) mutant virus. Furthermore, the contribution of US1 gene products to the loss of
253 cellular MR1, confirms that more than one viral product contributes to the early loss of MR1 protein.
254 To test whether the early loss of mRNA is reflected in a corresponding reduction in MR1 protein, ARPE-
255 19 MR1-GFP cells were infected with HSV-1 17syn⁺ and 17(41-) strains, optionally treated with MR1
256 ligand at 3 h p.i., and then harvested 3 hours later. Regardless of ligand treatment there was a
257 reduction in MR1-GFP at this early timepoint, which was partially rescued in cells infected with the
258 vhs mutant (Fig. 5.B). In parallel, ARPE-19 cells were similarly infected and stained for the late HSV-1
259 glycoprotein gD. Expression of the viral glycoprotein gD was slightly higher in cells infected with the

260 17(41-) mutant compared to the parental 17syn+ strain (Fig. 5.A). This confirmed that delayed
261 expression kinetics in the 17(41-) mutant were not responsible for the partial rescue of MR1-GFP.

262 In conclusion, vhs expression is sufficient to downregulate endogenous and over-expressed MR1,
263 inhibiting the cell's ability to present MR1 ligand on the plasma membrane. This phenotype is driven
264 by an early loss of MR1 isoform transcripts. Despite the substantial loss of transcripts by late
265 timepoints, viral infection lacking vhs expression only partially rescues the loss of MR1 protein at early
266 but not late times post infection, confirming multiple viral products contribute to the modulation of
267 MR1.

268 **ICP22 and vhs expression downregulate MR1 in key sub-cellular** 269 **compartments**

270 As previously described, MR1 is predominantly ER-associated, with ligand availability triggering
271 maturation and egress through the secretory pathway. Once on the plasma membrane MR1
272 endocytoses and is predominantly degraded rather than recycled back to the surface membranes.^{51,80}
273 To further examine the effect of ICP22 and vhs on the loss of MR1 within cells, the relative amount of
274 MR1 in subcellular compartments in the secretory and endocytic pathways of adenovirus RAd-ICP22
275 and RAd-vhs infected ARPE-19 MR1-GFP cells was evaluated by high throughput fluorescence
276 microscopy. Cells were treated with ligand at the time of infection to promote MR1 maturation and
277 trafficking and then stained for the nucleus (DAPI), ER (calreticulin), Golgi apparatus (GA, GM130),
278 plasma membrane (wheat germ agglutinin), early endosomes (EEA1) or late endosomes/lysosomes
279 (LAMP1) at 30 h p.i.^{51,81} Expression of both viral proteins resulted in an overall reduction of MR1 within
280 cells, compared to that detected in the RAd-Ctrl control infected samples (Fig. 6.A). The pattern of
281 staining of subcellular compartments was unaffected by ICP22 and vhs expression compared to RAd-
282 Ctrl (Fig. 6.B). Ilastik machine learning software⁸² was trained to create a segmentation mask based
283 on the subcellular markers so that the median MR1-GFP signal in each field of view (FOV) could
284 compared to the RAd-Ctrl infected samples for a quantitative analysis. A significant reduction in MR1
285 was detected in the immature pool in the ER, the secretory pathway (GM130), the plasma membrane,
286 the endocytic (EEA1) and degradation pathways (LAMP1) (Fig. 6.C, E). The fold change of MR1-GFP
287 intensity was calculated for each subcellular compartment with respect to the median for the FOV to
288 establish whether all locations within the cell were equally depleted of MR1 protein (Fig. 6. D, F). The
289 pool of ER-resident MR1 was preferentially lost, although the relative reduction was modest. Levels
290 of MR1 in the GA was consistent with the median, while the plasma membrane and late
291 endosomes/lysosomes were slightly increased. Surprisingly there was a stronger relative reduction of
292 MR1 in the early endosomes, although the reason why these vesicles would be particularly depleted

293 is unclear. Other than this compartment, the relatively uniform reduction in MR1 within the cell is
294 consistent with loss emanating from a reduction of MR1 in the ER available to bind and traffic ligand
295 to the plasma membrane.

296 **HSV-2 modulation of MR1 mirrors HSV-1**

297 Herpes simplex virus type 2 is thought to have emerged by cross-species transmission around 1.6
298 million years ago.⁸³ Parallel evolutionary pressures from the shared host combined with low rates of
299 nucleotide substitution⁸³⁻⁸⁵ have minimised the extent of divergence in viral products between HSV-1
300 and HSV-2. Given that the third, less closely related alphaherpesvirus VZV also modulates MR1³⁸ the
301 ability of HSV-2 to modulate MR1 was examined. To that end ARPE-19 MR1-GFP cells were infected
302 with HSV-2 strain 186 (MOI 3), optionally treated with MR1 ligand 24 hours before infection (Pre), 14
303 hours post infection (Post) or left untreated (Nil) and then stained for surface MR1 at 18 h p.i. (Fig.
304 7.A). Total and surface MR1 were significantly downregulated in the absence of ligand and when cells
305 were ligand treated post infection. While significant loss of total MR1 was also evident when cells
306 were pre-treated with ligand, surface MR1 was comparable to mock infected cells, reflecting a
307 protection of pre-existing surface molecules from viral modulation also observed in MR1-GFP surface
308 expression during HSV-1 infection.³⁷ Interestingly, while HSV-2 infected ARPE-19 cells expressing the
309 wild type MR1 molecule were similarly depleted of surface MR1 both in the absence of ligand and
310 with post-infection treatment, surface MR1 was significantly upregulated with pre-infection ligand
311 treatment (Fig. 7.B). This was also observed with HSV-1 infection³⁷ suggesting the GFP tag may block
312 the upregulation of surface MR1 molecules during both HSV-1 and HSV-2 infection.

313 The one site of immature N-linked glycosylation on the MR1 α 1 extracellular domain is remodelled
314 into the mature form when the protein leaves the ER and traffics through the secretory pathway.
315 Digest of the MR1 protein by endoglycosidase H (Endo H) reduces the molecular weight of immature
316 but not the mature glycosylated form resulting in the detection of two separate MR1 bands by western
317 blot. ARPE-19 MR1 cells were infected with HSV-2 and treated with one of the three ligand conditions
318 as described above. Cell lysates were then digested with Endo H and probed for MR1, GAPDH (cellular
319 control) and ICP27 (viral control).

320 No MR1 was detected in the HSV-2 infected samples lacking ligand or treated at 14 h p.i., consistent
321 with the loss of both total and surface MR1 detected by flow cytometry under the same assay
322 conditions (Fig. 7.C). Only a faint band of Endo H resistant, mature MR1 (black arrow) remained in the
323 infected cells pre-treated with ligand, at a comparable strength to the uninfected samples, indicating
324 that only the mature, pre-existing MR1 is protected from downregulation by HSV-2.

325 To examine the impact of HSV-2 on MR1 mRNA HF cells were infected for 6 hours and the transcripts
326 amplified by RT-qPCR using the MR1A, MR1B and pan-specific MR1 primers. A significant reduction in
327 transcripts was detected using all three primer sets indicating that during HSV-2 infection loss of MR1
328 transcripts contributes to the reduction in MR1 protein (Fig. 7.D). Together this data demonstrates
329 that HSV-2 infection mirrors the HSV-1 induced MR1 phenotype characterised by the early loss of
330 MR1A, B and total MR1 transcripts, near complete loss of immature MR1 protein with only mature
331 and surface MR1 protected from HSV-2 downregulation.

332 **Relative retention of MR1 on plasma membrane during HSV-1 and HSV-2** 333 **infection**

334 Although the loss of MR1 in HSV-1 and HSV-2 infected epithelial cells is pronounced, it is not uniformly
335 lost within the cell, given the retention of mature Endo H resistant forms (Fig. 6.B).³⁷ To further
336 examine the effect of infection on the loss of MR1 within the subcellular compartments in the
337 secretory and endocytic pathways, HSV-1 and HSV-2 (MOI 5) infected ARPE-19 MR1-GFP cells were
338 stained and examined by fluorescence microscopy at 6 h p.i. as previously described. Given that there
339 was no detectable modulation of surface MR1 by flow cytometry (Figures 5 and 7) the MOI was
340 increased to 5 to promote a more rapid transition through the viral expression cascade. Cells were
341 pre-treated with ligand for 16 h prior to infection to promote MR1 maturation and trafficking. The
342 contribution of vhs to the loss of MR1 was explored by comparing the HSV-1 17(41-) vhs mutant to
343 the parental strain 17syn+.

344 The staining of subcellular compartments in the infected cells was qualitatively consistent with Mock
345 infected cells (Fig. S1), lacking the marked rearrangement of cellular markers and cytoplasmic effect
346 that is characteristic of later stages of infection.⁸⁶ Within the FOV cell mask MR1 was significantly
347 downregulated in HSV-2 and HSV-1 cells, with the loss partially recovered in the absence of vhs
348 expression (Fig. 8.A, C). There was an absolute loss of MR1 in each subcellular compartment, although
349 the loss from the plasma membrane associated with HSV-2 infection was modest and the vhs mutant
350 similarly had limited impact on EEA1-associated MR1. Furthermore, there was a partial recovery
351 associated with the vhs mutant in all compartments other than the plasma membrane, where the
352 downregulation was consistent between parental strain and vhs mutant.

353 The relative amount of MR1-GFP within each subcellular compartment with respect to the median for
354 the FOV was also calculated, and then expressed as a fold change to the proportion detected in the
355 control infected cells (Fig. 8.B, D). MR1 in the ER, GA and late endosomes/lysosomes was more
356 strongly depleted compared to the median within the FOV, with the vhs mutant mediating a relative
357 recovery of MR1 only in late endosomes. By contrast, MR1 on the plasma membrane was instead

358 retained (HSV-2, 17(41-)) or upregulated (HSV-1 17syn+). Similarly there was no relative reduction in
359 the EEA1 labelled compartments (Fig. 8.E) associated with HSV-1, HSV-1 17syn+ or 17(41-) viral
360 infections.

361 While there is some consistency at this early timepoint post infection with the absolute and relative
362 reduction of MR1 within cellular compartments resulting from the expression of ICP22 and vhs, there
363 are also some interesting differences. Both models drive a relatively stronger loss of MR1 from the ER,
364 even when the virus lacks vhs expression. However, viral infection, including from the vhs mutant,
365 results in a similarly stronger relative loss of MR1 from the GA which was not evident with ectopic
366 ICP22 or vhs protein expression. Furthermore viral infection failed to preferentially target loss of MR1
367 from early endosomes, with some of the punctate cytoplasmic accumulations colocalizing with EEA1.
368 Consistent with the finding that vhs expression preferentially targeted the EEA1 associated MR1, there
369 was a significant recovery in the absolute amount of MR1 with the vhs mutant. Together these results
370 indicate that during the initial hours post infection MR1 is preferentially lost from the ER pool,
371 secretory and degradation pathways but other mechanism(s) may impact the amount of MR1 on the
372 plasma membrane and in early endocytic compartments.

373 Discussion

374 This study identifies several herpes simplex virus gene products that modulate MR1 expression;
375 specifically the IE proteins ICP22 and US1.5, and the viral RNase vhs. It also establishes impacts on
376 MR1 transcription by vhs, and protein degradation mediated by ICP22, and to a lesser extent the
377 shorter gene product US1.5. Finally it demonstrates that an additional alphaherpesvirus, HSV-2, also
378 targets MR1 expression. Although the impact of the multifaceted modulation of this key resident
379 immune cell population is not explicitly examined, delayed and diminished MAIT cell effector capacity
380 is likely to impact viral clearance and MAIT cell cytolytic killing of virally infected cells, thus promoting
381 more efficient establishment of viral latency and transmission to a new host.

382 Cellular MR1 is progressively reduced during the first 6 hours of infection³⁷ placing IE gene products
383 high on the list of candidates. Infection with a virus lacking expression of the IE protein ICP0, an E3
384 ubiquitin ligase responsible for degradation of various cellular proteins^{42,87-89} failed to rescue the
385 phenotype.³⁷ A second candidate ICP47, responsible for blocking peptide loading into the antigen cleft
386 of MHC-I molecules was initially dismissed, given that early studies found that MR1 could present
387 antigen independent of TAP, the member of the peptide loading complex (PLC) that controls import
388 of the peptides into the ER lumen.^{90,91} Furthermore, ectopic expression of ICP47 in human dendritic
389 cells and lung epithelial cells fails to inhibit interferon- γ secretion by MR1-restricted T cell clones in
390 response to mycobacteria tuberculosis challenge.⁹² However, a more recent study revealed that MR1
391 is stabilised in the ER by the PLC,⁴⁷ warranting examination of the effect of ICP47 binding. HSV-1
392 infection of epithelial cells overexpressing MR1-GFP with a virus lacking ICP47 expression however
393 failed to rescue the loss of total or surface MR1 at either early or late timepoints (Fig. 1) demonstrating
394 that this viral protein modulates MHC-I but not MR1 antigen presentation.

395 A third IE protein ICP22, encoded by the US1 gene, was screened due to its multifaceted control of
396 cellular and viral transcription, involvement in protein quality control,⁵⁷ and the demonstrated
397 capacity of the HSV-2 homolog to act as an E3 ubiquitin ligase.⁶⁴ Although ICP22 is predominantly
398 nuclear in location,⁹³ ICP22 expression reduces the aggregation of non-native proteins in the
399 cytoplasm, confirming that its localisation is not restricted to the nucleus.⁵⁷ Ectopic plasmid expression
400 of HSV-1 ICP22 resulted in a downregulation of endogenous surface MR1. While the full length protein
401 induced a strong reduction in MR1, the shorter US1.5 protein demonstrated a more limited loss based
402 on the MR1-GFP signal detected by flow cytometry, although there was substantial loss of MR1
403 resulting from expression of both constructs detected by immunoblot (Fig. 2). Inhibition of
404 proteasomal and lysosomal protein degradation established that US1 gene products promote
405 proteasomal degradation of MR1, consistent with the loss of MR1 from the ER, GA, plasma membrane,

406 early and late endocytic compartments with ectopic ICP22 expression (Fig. 6). This significant finding
407 explains the MG132 mediated rescue of MR1 protein during HSV-1 infection,³⁷ and represents an
408 additional immunomodulatory function of the US1 gene.

409 The differential strength of the modulation between ICP22 and US1.5 suggests that the N-terminal
410 domain may be required for optimal modulation of MR1. Interestingly, the N-terminal domain is
411 proposed as the site of Hsc70 interaction associated with protein quality control functionality.⁵⁷
412 However, a definitive understanding of the functional overlap between ICP22 and US1.5 is
413 complicated by the lack of agreement over whether US1.5 translation commences from residues 90,
414 157^{58,65} or 171 as was used in this study.^{60,66}

415 ICP22 acts as a trans-regulator to promote late viral gene expression, consequently ICP22 null mutants
416 demonstrate attenuated viral replication, impaired expression of vhs (Ng et al., 1997), and progeny
417 containing reduced amounts of some glycoproteins⁹⁴⁻⁹⁶. This complicates evaluating the contribution
418 of US1 gene products to MR1 modulation through infection with an US1 null virus.

419 Although this study demonstrates that ectopic expression of both ICP22 and US1.5 are sufficient to
420 downregulate MR1 expression, future studies are required to identify how ICP22 promotes MR1
421 proteasomal degradation, evaluate the HSV-2 homologs, and confirm the contribution of ICP22 and
422 US1.5 to the loss of MR1 in the context of viral infection.

423 HSV-1 and HSV-2 both encode homologs of the potent viral RNase vhs that contribute to
424 pathogenesis.⁹⁷⁻¹⁰⁰ Vhs effectively suppresses multiple arms of the innate and antiviral response
425 including blocking detection of viral DNA,¹⁰¹ interferon signaling pathways,¹⁰² interferon stimulated
426 gene expression¹⁰³⁻¹⁰⁵ and inactivation of dendritic cells.¹⁰⁶ In this study we extend the list of antigen
427 presentation molecules downregulated by vhs from MHC-I and MHC-II^{107,108} to also include MR1.
428 Interestingly UV-inactivated HSV-1 effects a modest but significant reduction in surface MR1 which
429 could be derived from vhs released from the tegument of infecting viral particles.³⁷ HSV-1 vhs
430 expressed from an adenovirus construct effected a reduction in cellular MR1-GFP in ARPE-19 cells,
431 and consequently failed to upregulate surface MR1 in response to ligand treatment. Consistent with
432 this result, MR1 was lost from all 5 of the subcellular locations examined from fluorescent microscopy
433 (Fig, 6), reflecting loss of MR1 emanating from the earliest stage in the MR1 biosynthesis pathway.

434 Four different protein isoforms are synthesised from the *mr1* gene through differential splicing.⁷⁴
435 While the MR1A isoform is relatively well characterised as the membrane-bound form that presents
436 ligands to MAIT cells, there is evidence suggesting the MR1B isoform may prevent MAIT cell response
437 to non-pathogenic levels of riboflavin biosynthesis through ligand binding to MR1B homodimers

438 retained in the ER.^{75,76} Using primers designed to detect MR1A, B and total transcripts the levels of
439 endogenous and MR1A overexpressed transcripts were examined at three timepoints following
440 infection (Fig. 4). HSV-1 infection resulted in a downregulation of overexpressed and endogenous MR1
441 transcripts by 2 and 6 h p.i. respectively. Using MR1A and MR1B specific primers it was confirmed that
442 in HF cells, endogenous levels of both were depleted by 6 h p.i., but that infection with the vhs 17(41-
443) deletion mutant rescued the loss of both isoforms and the combined MR1 transcripts to those of
444 mock infected cells.

445 Multiple HSV gene products have global impacts on transcripts, including vhs, ICP4, ICP22 and the
446 ICP27-mediated disruption of transcription termination.¹⁰⁹ Unexpectedly, deletion of the short non-
447 coding RNA sequence sncRNA1 from the HSV-1 genome drives increased MR1 transcript levels in the
448 trigeminal ganglia of mice after ocular infection.¹¹⁰ Currently, there is an extremely limited
449 understanding of the factors affecting regulation of the ubiquitously expressed MR1 gene, although it
450 has been shown to vary between cell types,¹¹¹ is upregulated by inflammatory cytokines associated
451 with type 1 diabetes,¹¹² and the ratio of MR1A to MR1B isoforms varies between tissues and
452 individuals.⁷⁶ One publication that has examined MR1 transcripts during viral infection detected
453 elevated MR1 transcripts in hepatocytes infected with hepatitis B virus, with an associated increase in
454 cytotoxicity of MAIT cells.¹¹³ Although vhs facilitates the degradation of many host transcripts,
455 infection of the ARPE-19 MR1-GFP cells with the vhs mutant 17(41-) demonstrated a complete rescue
456 of MR1 transcripts (Fig. 4.C) and a partial rescue of the loss of total cellular MR1 protein at 6 h p.i. (Fig.
457 5.B). This suggests that vhs is the dominant mechanism of MR1 mediated loss of MR1 transcripts, and
458 that this contributes to the modulation of MR1 antigen presentation during HSV-1 infection. A more
459 thorough investigation of the effects of HSV-1 products on MR1 promoter activity and transcript
460 longevity would be of additional interest.

461 Given that HSV-1, VZV and HCMV all modulate MR1 antigen presentation,^{37,38} HSV-2 was also
462 examined and found to be capable of modulating MR1 in a ligand-dependent fashion that mirrored
463 the HSV-1 induced phenotype. Furthermore, lower levels of MR1A, MR1B and total MR1 transcripts
464 were detected in HSV-2 infected cells (Fig. 7.D), potentially implicating HSV-2 vhs in the modulation
465 of MR1. During HSV-1 infection of ARPE-19 MR1 cells, we have previously published immunoblots
466 demonstrating that loss of MR1 progressively increases during the first 6 hours post infection.³⁷ Any
467 future study that examines the contribution of HSV-2 gene products to the modulation of the MR1,
468 including the HSV-2 vhs ICP22 and US1.5 homologs, may benefit from such an examination.

469 Interestingly, both HSV-1 and HSV-2 infection promoted increased surface MR1 when cells were pre-
470 treated with Ac-6-FP ligand however there was no significant difference in the abundance of the GFP-

471 tagged molecule with either virus compared to mock-infected cells.³⁷ Recently it was shown that MR1
472 endocytosis occurs via AP2 recognition of its C-terminal cytoplasmic tail.⁸⁰ Interestingly, the C-terminal
473 fusion of MR1 with GFP resulted in reduced endocytosis likely due to the GFP molecule preventing
474 AP2 binding to the tail.³⁷ Therefore it is possible that the increased cell surface stability of MR1, but
475 not MR1-GFP molecules, is due to HSV interrupting AP2-mediated endocytosis of MR1; however this
476 remains to be investigated.

477 As previously discussed, expression of both HSV-1 ICP22 and vhs proteins resulted in a cell-wide
478 reduction in MR1 however manipulation of ligand timing during HSV-1³⁷ and HSV-2 infection revealed
479 retention of some mature Endo H resistant protein. To further examine the relative pattern of
480 intracellular loss ARPE-19 MR1-GFP cells were pretreated with ligand to promote MR1-GFP
481 distribution, infected with HSV-1 or HSV-2, and then examined by fluorescence microscopy at 6 h pi.
482 Even at this early time point there was loss from the ER, GA, plasma membrane, and early and late
483 endocytic compartments (Fig. 8). Cells similarly infected with the HSV-1 vhs mutant virus
484 demonstrated a partial restoration of MR1 from each compartment resulting from the recovery of
485 transcripts. Unlike that observed with ectopic ICP22 and vhs expression, MR1 associated with EEA1-
486 labelled compartments was downregulated at levels comparable to the whole cell. Furthermore,
487 surface MR1 was relatively elevated compared to the median cellular MR1 in the HSV-1 17Syn+
488 infected cells suggesting that additional factors modulate localisation of mature MR1 during viral
489 infection.

490 In conclusion, these findings increase our understanding of the mechanisms employed by HSV-1 to
491 protect against the targeted MR1-dependent attack by resident MAIT cells by establishing that during
492 HSV-1 infection vhs targets MR1 transcripts while ICP22 targets MR1 for proteasomal degradation. In
493 addition, we establish that HSV-2 also downregulates MR1, further implicating the MR1 antigen
494 presentation pathway as a target conserved across multiple herpesviruses.

495 **Limitations of Study**

496 This study utilised GFP-tagged overexpressed MR1 to assess the modulation of MR1 protein in
497 intracellular compartments during herpes simplex virus infection, and resulting from the ectopic
498 expression of the HSV-1 US1 and UL41 viral gene products. Given that addition of the C-terminal GFP
499 tag slightly delays MR1 endocytosis,⁸⁰ evaluation of the localisation of untagged MR1 under the same
500 experimental conditions would be of interest, however, comparisons would need to take into
501 consideration that a pan-MR1 antibody capable of detecting all conformations of the MR1 are
502 currently unavailable.

503 The loss of total MR1 by ectopic expression of ICP22 or US1.5 was rescued by treatment with
504 proteasomal inhibitor MG132. Additional research is required to confirm whether these viral proteins
505 promote proteasomal degradation of MR1 through direct interaction with MR1, or whether they
506 encode ubiquitin ligase functionality.

507 The study did not examine vhs, ICP22 or US1.5 from HSV-2, so it is not possible to conclude that they
508 modulate MR1 in line with that observed with their respective HSV-1 homologs. This requires
509 independent investigation.

510 **Acknowledgments**

511 C.S. and T.V. were each supported by an Australian Postgraduate Award/Australian Government
512 Research Training Program Scholarship. We acknowledge grant support from the National Health
513 and Medical Research Council (NHMRC) of Australia: 198704 (A.A. and B.S.), 2003192 (H.E.G.M.),
514 and 1113293 and 1154502 (J.A.V.), the US National Institutes of Health RO1 R01AI148407 (J.R. and
515 J.A.V.), NHMRC Leadership Investigator grants 2008913 (J.R.), and 2016969 (JAV), Australian
516 Research Council (ARC) DP170102471 (J.A.V.), Wellcome Trust 204870/Z/16/Z (R.J.S.) and UK
517 Medical Research Council (MRC) MR/S00971X/1 (R.J.S.).

518

519 The authors wish to thank members of the Herpesvirus Pathogenesis and Viral Immunology research
520 groups (School of Medical Sciences, The University of Sydney) for helpful discussions and acknowledge
521 the Sydney Cytometry Core Research Facility, a joint initiative of Centenary Institute and the University
522 of Sydney, for assistance with flow and imaging cytometry experiments.

523 **Author Contributions**

524 Conceptualization, C.S.; methodology, C.S., H.E.G., B.P.M, J.G.B; formal analysis, C.S.; resources, T.V.,
525 D.C.T., J.R., R.S., J.A.V.; writing—original draft, C.S.; writing—review & editing, A.A., B.S.; funding
526 acquisition, A.A., B.S. All authors have read and agreed to the published version of the manuscript.

527 **Declaration of interests**

528 The authors declare that the research was conducted in the absence of any commercial or financial
529 relationships that could be construed as a potential conflict of interest.

530 **Figure Titles and Legends**

531 **Figure 1. HSV-1 ICP47 deletion mutant fails to rescue loss of MR1.** (A) ARPE-19 cells were mock (black),
 532 HSV-1 strain KOS (red) or ICP47del mutant lacking expression of ICP47 (blue) infected (MOI 3) in parallel.
 533 Cells were harvested at 6 h p.i. and stained for viral glycoprotein gC or matching isotype control (grey) and
 534 analysed by flow cytometry. Histograms representative of two independent experiments. (B, C, D) ARPE-
 535 19 MR1-GFP cells were mock (black), HSV-1 strain KOS (red) or ICP47del (blue) infected in parallel. (B, C)
 536 Cells were treated with Ac-6-FP (5 μ M) at 3 h p.i. before harvesting at 6 h p.i. (D) or treated at 14 h p.i.,
 537 before harvesting at 18 h p.i. Cells were stained for surface MHC-I (B) or surface MR1 (C, D) or matching
 538 isotype control (grey) and analysed by flow cytometry. Fold change in MFI of infected cells relative to mock
 539 infected cells (dotted black line) is represented as mean \pm SEM. Statistical significance was calculated by
 540 paired Student's t-test * $p < 0.05$, ** $p < 0.005$, **** $p < 0.0001$. Analysis of 4 or 5 independent experiments.
 541

542 **Figure 2. ICP22 expression modulates loss of total and surface MR1.** (A) 293T cells were transfected with
 543 a plasmid encoding either GFP alone (pSY10, black) or GFP and HSV-1 US1 gene (pSY10-ICP22, green). Cells
 544 were treated with Ac-6-FP (5 μ M) 22 h post transfection and harvested 6 hours later. Cells were stained
 545 for surface MR1 or MHC-I and analysed by flow cytometry. Fold change in MFI relative to GFP⁻ cells (dotted
 546 line) within each sample was calculated and is represented as mean \pm SEM. Statistical significance
 547 compared to pSY10 was evaluated by Welch's unpaired t-test ** $p < 0.005$, **** $p < 0.0001$. Analysis of 6 or
 548 7 independent experiments. (B) ARPE-19 MR1-GFP cells were infected with RAd-Ctrl adenovirus (black or
 549 dotted line) or RAd-Ctrl modified to encode HSV-1 US1 gene (RAd-ICP22, green) or HSV-1 US1.5 gene (RAd-
 550 US1.5, orange), MOI 100. Cells were left untreated (Nil) or treated with Ac-6-FP (5 μ M) for 4 hours prior to
 551 harvesting at 44 h p.i. (Post). Cells were stained for surface MR1, MHC-I or matching isotype control (grey)
 552 and analysed by flow cytometry. Fold change in MFI of live infected cells relative to RAd-Ctrl with matching
 553 ligand treatment is represented as mean \pm SEM. Statistical significance was calculated by paired Student's
 554 t-test, * $p < 0.05$, ** $p < 0.005$, **** $p < 0.0001$. Analysis of 4 independent experiments. (C) ARPE-19 MR1 cells
 555 were infected with RAd-Ctrl, RAd-ICP22 or RAd-US1.5 or mock infected. Cells were harvested at 44 h p.i.
 556 and lysates were separated by gel electrophoresis before immunoblotting for MR1, MHC-I, GAPDH and
 557 FLAG to detect expression of the viral gene. Faint GAPDH band from prior probe denoted *. (D, E) ARPE-19
 558 MR1-GFP cells were infected with RAd-Ctrl (black), RAd-ICP22 (green) or RAd-US1.5 (orange), MOI 100 for
 559 46 hours. Cells were treated with proteasomal inhibitor MG132 (5 μ M), lysosomal inhibitor folimycin (50
 560 nM) or DMSO vehicle control (1:400) for a further 16 hours prior to harvest and analysis by (D) flow
 561 cytometry or (E) immunoblot. (D) Fold change of total MR1 (GFP) was detected by flow cytometry
 562 (inhibitor:DMSO) in live cells for each adenovirus, and is represented as mean \pm SEM. Statistical
 563 significance was calculated by paired Student's t-test, * $p < 0.05$. Analysis of 4 independent experiments. (E)
 564 Lysates were separated by gel electrophoresis before immunoblotting for GAPDH and FLAG to detect
 565 expression of the viral gene.
 566

567 **Figure 3. HSV-1 vhs protein expression modulates loss of total and surface MR1.** (A) ARPE-19 MR1-GFP
 568 cells were infected with RAd-Ctrl adenovirus (black or dotted line) or RAd-Ctrl modified to encode HSV-1
 569 vhs (RAd-vhs, green), MOI 100. Cells were left untreated (nil) or treated with Ac-6-FP (5 μ M) for 4 hours
 570 prior to harvesting at 44 h p.i. (post). Cells were stained for surface MR1, MHC-I or matching isotype control
 571 (grey) and analysed by flow cytometry. Fold change in MFI of live infected cells relative to RAd-Ctrl with
 572 matching ligand treatment is represented as mean \pm SEM. Statistical significance was calculated by paired
 573 Student's t-test, * $p < 0.05$, **** $p < 0.0001$. Analysis of 4 independent experiments. (B) ARPE-19 MR1 cells

574 were infected with RAd-Ctrl adenovirus or RAd-vhs or mock infected. Cells were harvested at 44 h p.i. and
 575 lysates were separated by gel electrophoresis before immunoblotting for MR1, MHC-I, and GAPDH.

576

577 **Figure 4. HSV-1 infection downregulates MR1 transcripts.** (A) HF and (B) ARPE-19 MR1 cells were mock or
 578 HSV-1 strain F infected in parallel (MOI 5). Cell lysates were harvested at 2, 6 or 16 h p.i., and mRNA levels
 579 for MR1 and 18s were evaluated by RT-qPCR. (C) HF cells were infected with HSV-1 strains 17syn+ (red) or
 580 17(41-) lacking expression of vhs (blue) or mock infected in parallel. Cells were harvested at 6 h p.i. and
 581 mRNA levels of MR1A, MR1B, combined MR1 isoforms and 18s were evaluated by RT-qPCR. (A, B, C) Fold
 582 change compared to mock infection was calculated after normalising to levels of 18s and is represented as
 583 mean +/- SEM. Statistical significance to mock (dotted line) for MR1 was calculated by paired Student's t-
 584 test * p<0.05, ** p<0.005, *** p<0.0005, **** p<0.0001. Analysis of 3 independent experiments.

585

586 **Figure 5. HSV-1 vhs deletion mutant partially recovers loss of total MR1-GFP.** (A) ARPE-19 cells were mock
 587 (black), HSV-1 strains 17syn+ (red) or 17(41-) (blue) infected in parallel (MOI 3). Cells were harvested at 6
 588 h p.i. and stained for late viral glycoprotein gD or matching isotype control (grey) and analysed by flow
 589 cytometry. Histograms representative of two independent experiments. (B) ARPE-19 MR1-GFP cells were
 590 mock (black), HSV-1 strains 17syn+ (red) or 17(41-) (blue) infected in parallel. Cells were left untreated (nil)
 591 or treated with Ac-6-FP (5 µM) at 3 h p.i. (post) before harvesting at 6 h p.i. Total MR1 (GFP) was detected
 592 by flow cytometry. Fold change in MFI of infected cells relative to mock infected cells with matching ligand
 593 treatment is represented as mean +/- SEM. Statistical significance was calculated by paired Student's t-test
 594 * p<0.05. Analysis of 3 independent experiments.

595

596 **Figure 6. ICP22 and vhs expression downregulate MR1 in key sub-cellular compartments.** ARPE-19 MR1-
 597 GFP cells were infected with RAd-Ctrl adenovirus (white) or RAd-Ctrl modified to encode HSV-1 ICP22 (RAd-
 598 ICP22, red) or HSV-1 vhs (RAd-vhs, orange), MOI 100. Cells were treated with Ac-6-FP (5 µM) at time of
 599 infection. Cells were stained at 30 h p.i. with wheat germ agglutinin (WGA) (plasma membrane) and then
 600 permeabilised and stained for calreticulin (ER), GM130 (Golgi apparatus), EEA1 (early endosomes) or
 601 LAMP1 (late endosomes/lysosomes) and DAPI (nucleus). (A) Representative images of MR1-GFP and (B)
 602 images of DAPI and WGA (white) merged with calreticulin, GM130, EEA1 or LAMP1 (magenta) from two
 603 independent experiments. Scale bar 50 µm. Cell segmentation completed with ilastik software and
 604 quantification of fold change of MR1 intensity relative to RAd-Ctrl (C, E) or total cellular MR1 within each
 605 field of view (FOV) (D, F) performed with ImageJ software. Violin plots of individual fold change points are
 606 depicted with median + quartiles. Statistical significance was calculated with one-way ANOVA, * p<0.05,
 607 **** p<0.0001. Analysis of at least 14 FOV in two independent experiments.

608

609 **Figure 7. HSV-2 targets immature MR1 protein while ligand-bound mature MR1 is protected.** (A) ARPE-
 610 19 MR1-GFP or (B, C) ARPE-19 MR1 cells were mock or HSV-2 infected in parallel (MOI 3). Cells were either
 611 left untreated (Nil) or treated with Ac-6-FP (5 µM) for 24 h prior to infection (Pre) or at 14 h p.i. (Post)
 612 before harvesting at 18 h p.i. (A, B) Cells were stained for surface MR1 or isotype control (grey) and
 613 analysed by flow cytometry. Fold change in MFI of infected cells (red) relative to mock infected cells (black)
 614 with matching ligand treatment is represented as mean +/- SEM. Statistical significance was calculated by
 615 paired Student's t-test * p<0.05, ** p<0.005, *** p<0.0005, **** p<0.0001. (C) Cell lysates were left
 616 undigested or EndoH digested before immunoblotting for MR1, GAPDH, GFP or ICP27. Endo H resistant
 617 MR1 is denoted with black triangle while Endo H susceptible bands denoted with blue triangle. Red star
 618 denotes retained EndoH resistant band in HSV-2 infected cells pre-treated with ligand. (D) HF cells were

619 infected with HSV-2 or mock infected in parallel. Cells were harvested at 6 h p.i. and mRNA levels of MR1A,
620 MR1B, combined MR1 isoforms and 18s were evaluated by RT-qPCR. Fold change compared to mock
621 infection was calculated after normalising to levels of 18s, represented as mean +/- SEM. Statistical
622 significance to mock (dotted line) for MR1 was calculated by paired Student's t-test ** $p < 0.005$, ***
623 $p < 0.0005$, **** $p < 0.0001$. Analysis of 1 (C) or 3 (A, B, D) independent experiments.

625 **Figure 8. HSV-1 and HSV-2 mediated loss of MR1 is strongest in the ER and secretory pathway and is**
626 **partially recovered in absence of vhs expression.** ARPE-19 MR1-GFP cells were infected (MOI 5) with HSV-
627 2 (orange), HSV-1 strains 17syn+ (red) or 17(41-) lacking expression of vhs (blue) or mock (white) infected
628 in parallel. Cells were treated with Ac-6-FP (5 μ M) for 16 h prior to infection. Cells were stained at 6 h p.i.
629 with wheat germ agglutinin (WGA) (plasma membrane) and then permeabilised and stained for calreticulin
630 (ER), GM130 (Golgi apparatus), EEA1 (early endosomes) or LAMP1 (Late endosomes/lysosomes) and DAPI
631 (nucleus). Cell segmentation completed with ilastik software and quantification of fold change (FC) in MR1
632 intensity relative to mock (A, C) or total cellular MR1 within each field of view (FOV) (B, D) performed with
633 ImageJ software. Violin plots of individual fold change points are depicted with median + quartiles.
634 Statistical significance was calculated with one-way ANOVA, * $p < 0.05$, ** $p < 0.005$, *** $p < 0.0005$, ****
635 $p < 0.0001$. Analysis of at least 14 FOV in two independent experiments. (E) Representative images of DAPI
636 + WGA, MR1-GFP, EEA1 and merged images with white arrows highlighting examples of colocalization in
637 enlarged image (box) on right. Scale bar 50 μ m.

638 STAR METHODS

639 RESOURCE AVAILABILITY

640 Lead contact

641 Further information and requests for resources and reagents should be directed to and will be
642 fulfilled by the Lead Contact, Barry Slobedman (barry.slobedman@sydney.edu.au).

643 Materials availability

644 Cells, viral mutants and constructs are available upon request, subject to our institutional and
645 Material Transfer Agreements, and those with the host institution at which these reagents were
646 generated.

647 Data and code availability

- 648 • All data reported in this paper will be shared by the lead contact upon request.
- 649 • This paper does not report original code.
- 650 • Any additional information required to reanalyze the data reported in this paper is available
651 from the lead contact upon request.

652 EXPERIMENTAL MODEL AND STUDY PARTICIPANT DETAILS

653 **Cells**

654 Human fibroblasts HF, human retinal pigment epithelial (ARPE-19), 293T, 293A and ARPE-19 cell lines
655 (all ATCC) expressing MR1 with co-expressed EGFP from the same promoter via a downstream internal
656 ribosomal entry site or MR1-GFP, both under the control of the Murine stem cell virus LTR,³⁷ Vero
657 (ATCC) and T-REx™-293 (ThermoFisher) cells were grown at 37°C and 5% CO₂ in Dulbecco's Modified
658 Eagle's Medium (Lonza) supplemented with 10% foetal calf serum (FCS, Cytiva). The sex of each cell
659 line is listed in the Key Resources Table. Cell lines have not been authenticated by ourselves.

660 **Viruses**

661 HSV-1 and HSV-2 strains used in this study were HSV-2 strain 186 (courtesy Dr Naomi Truong, The
662 Westmead Institute for Medical Research),¹¹⁴ HSV-1 strain F (courtesy Dr Russell Diefenbach,
663 Macquarie University), HSV-1 17syn+ (Prof Roger Everett, University of Glasgow), HSV-1 17syn+ vhs
664 mutant 17(41-) (Prof Roger Everett, University of Glasgow),⁷⁹ HSV-1 KOS (courtesy Prof P Kinchington,
665 University of Pittsburgh) and US12 (ICP47) null mutant ICP47del.⁴⁸

666 Cells were infected with HSV-1 or HSV-2 and mutant herpes viruses after replacing media for a 1 hour
667 period of adsorption (37°C), then washed and the media replaced. All HSV strains were grown and
668 titrated on Vero cells.

669 Replication deficient adenovirus constructs were generated from the pAdZ5-C5 vector.⁶⁷
670 Adenoviruses used in this study were: RAd-Ctrl (no exogenous protein-coding region),⁶⁷ RAd-ICP22,
671 RAd-US1.5, and RAd-vhs expressing the corresponding gene encoded by HSV-1 (strain F). Two-step
672 PCR using Q5 High-Fidelity polymerase (NEB) was used to amplify the viral genes adding either an N-
673 terminal FLAG tag (US1 and US1.5) or a C-terminal V5 tag (UL41 gene), with the second round of
674 amplification adding approximately 80 bp of homology to the vector construct. Primers are listed in
675 Table S1, with the gene-specific sequence underlined. SW102 *E. coli* containing the pAdZ5-C5 vector
676 were grown in low salt LB with ampicillin (50µg/ml) at 32 °C, shaking, until growth was exponential.
677 Lambda red proteins were induced by incubation at 42 °C for 15 mins, cooled on ice for 15-20 mins
678 and centrifuged to isolate the cell pellet. The gel-purified PCR product was added to the competent
679 SW102 cells which were electroporated in 0.2cm cuvettes at 2.50 kV. After recovery in LB (32 °C,
680 shaking for 4 hours) they were plated onto LB agar containing sucrose (5%), chloramphenicol (12.5
681 µg/ml), IPTG (200 µM) and Xgal (80 µg/ml) and then incubated for 30-48 hours at 32°C. Several white
682 colonies for each gene were selected for screening by incubating overnight (32°C, shaking) in LB
683 containing chloramphenicol (12.5 µg/ml). DNA was purified (QIAGEN) using 2-propanol to precipitate

684 the DNA, before redissolving the DNA in 10mM Tris pH 8.5. The sequence of each adenovirus insert
685 was confirmed by Sanger sequencing and CLC Genomics workbench (QIAGEN).

686 Confirmed constructs were purified (Macherey-Nagel) and transfected into T-REx™-293 cells using
687 FuGene HD (Promega). After several days the infected cells were collected, and the pellet lysed by
688 resuspending in equal volumes of PBS and tetrachloroethylene. After centrifugation the upper layer
689 of PBS containing the adenovirus was removed and stored at -80 °C. Virus was titrated after 48 h
690 infection in T-REx™-293 cells using goat anti-Adenovirus primary antibody (Sigma-Aldrich), anti-goat
691 HRP secondary antibodies and DAB substrate (Pierce).

692 **Plasmid expression constructs**

693 Primers (Forward: 5' **GTCTAC**ACTAGT**ATGGCCGACATTTCCCCAGG** 3'; reverse: 5'
694 **GTCTAC**AGATCT**CGGCCGGAGAAACGTGTCGCTG** 3'; US1 sequence underlined, restriction sites in bold)
695 were used to amplify the HSV-1 (Strain F) US1 sequence excluding the stop codon with Q5 High-Fidelity
696 polymerase (NEB). PCR products were purified and digested (SpeI-HF and BglII, NEB). The plasmid
697 backbone (pCDH_EF1-MCS-T2A-copGFP vector, Systems Bioscience) was digested (XbaI and BamHI-
698 HF, NEB), purified and ligated to the US1 fragment (NEB) to create the pSY10-ICP22 plasmid. This was
699 transformed into 5-alpha *E. coli* (NEB), selected on LB agar with ampicillin (50 mg/ml) and purified
700 (Macherey-Nagel). Sequence was confirmed by Sanger sequencing and CLC Genomics workbench
701 (QIAGEN). 293T cells were transfected with 1 µg parental plasmid (pSY10) or pSY10-ICP22 using
702 FuGene HD (Promega).

703 **METHOD DETAILS**

704 **Quantitative Reverse Transcription Polymerase Chain Reaction (qRT-PCR)**

705 Total RNA was extracted (Meridian Bioscience) prior to cDNA synthesis and quantitative polymerase
706 chain reaction (qPCR) (Aligent Technologies, Roche LightCycler®480 Instrument II PCR machine). PCR
707 settings were as follows: 10 min at 95 °C for denaturation, then 45 amplification cycles of 30 s at 95
708 °C, 40 s at 57 °C and 20 s at 72 °C, and the melt curve data was generated through 1 min at 95 °C, 30
709 s at 50 °C, 30 s at 95 °C. Test gene mRNA levels were normalised to mRNA levels of the housekeeping
710 gene 18s¹¹⁵ using the $\Delta\Delta CT$ method. Primers used for RT-qPCR are listed in Table S2.

711 **Immunoblotting**

712 Cells were harvested in cell lysis buffer (50 mM NaCl, 50 mM TRIS pH8, 1% IGEPAL, 1% Triton X-100)
713 supplemented with protease inhibitor cocktail (Sigma) and allowed to incubate on ice for 20 min.

714 Lysates were then centrifuged (16,000 x g for 20 min at 4 °C) and the supernatant collected. Lysates
715 were mock or Endo H (NEB) digested according to the manufacturer's instructions for 90 min at 37 °C
716 as required. Lysates were denatured by heating at 95 °C for 5 mins in reducing sample buffer (Bio-Rad)
717 and resolved by SDS- PAGE on precast polyacrylamide gels (Bio-Rad) before immunoblotting onto
718 PVDF membranes. Membranes were probed with the designated primary antibodies in 3% BSA in
719 PBST, followed by incubation with an appropriate horseradish peroxidase (HRP)-conjugated secondary
720 antibody (all Santa Cruz Biotechnology) and visualised using Clarity Western ECL Substrate (Bio-Rad).
721 The following primary antibodies were utilised: anti-MR1 CT,⁵¹ anti-MR1 (Abcam) and anti-HLA-A, B,
722 C (Abcam), anti-GFP (Santa Cruz Biotechnology), anti-GAPDH (Santa Cruz Biotechnology or
723 ThermoFisher), anti-DDDDK (anti FLAG, Abcam) and anti-ICP27 (Santa Cruz Biotechnology).
724 Immunoblots depicted in Figures 2.C and 3.B are from the same experiment and depict the same Mock
725 and RAd-Ctrl lanes. Unrelated samples were cropped from Figure 3.B.

726 **MR1 Ligand and Protein Degradation Inhibitors**

727 The MR1 ligand Acetyl-6-formylpterin (Ac-6-FP 5 µM, Schircks Laboratories) was added as indicated
728 to the culture medium. In the proteasomal and lysosomal inhibition assays, cells were treated with
729 MG132 (5µM, Sigma-Aldrich) or folimycin (50 nM Sigma-Aldrich) for 16 hours prior to harvest.

730 **Flow Cytometry**

731 The following antibodies were used to detect surface molecules: MHC-I by anti-HLA-A,B,C-PE (Miltenyi
732 Biotec), anti-HLA-A,B,C-APC (BD Pharmingen) or anti-HLA,B,C-SB436 (Invitrogen), HSV-1 gD by anti-
733 gD-FITC (Virostat) and HSV-1 gC by anti-gC (Virostat). Overexpressed MR1 was detected by anti-MR1
734 directly conjugated to PE or APC (Biolegend), while endogenous MR1 was detected by anti-MR1-biotin
735 (clone 26.5,⁵¹ followed by streptavidin conjugated to PE or APC (eBioscience). All cells were stained
736 for 20-30 minutes at 4 °C to minimise internalisation. Live cells were identified using Zombie NIR
737 Fixable Viability Kit (Biolegend) or Live/Dead™ Fixable blue (Invitrogen). Cells were fixed after staining
738 (BD Biosciences). Flow cytometry was performed using a LSR Fortessa X-20 or BD-LSR-II (BD
739 Biosciences) and data analysed using FlowJo software (Treestar Inc., <https://www.flowjo.com>, version
740 10.8).

741 **Fluorescence Imaging**

742 ARPE-19 MR1-GFP cells were seeded in duplicate on 96 well PhenoPlates (Perkin Elmer) precoated
743 with Geltrex™ basement membrane matrix (Gibco) and then infected as described with either HSV-1,
744 HSV-2 or adenovirus constructs. Cells were stained at 4 °C for delineation of plasma membrane (Wheat

745 Germ Agglutinin, CF405M Conjugate Biotium) in Hanks Balanced Salt Solution (Gibco) with 2% normal
746 donkey serum (Sigma-Aldrich). They were then fixed (BD Biosciences) and permeabilised and blocked
747 with the staining buffer (phosphate buffered saline, 1 mM CaCl₂/MgCl₂, 2% NDS) containing either
748 0.01% saponin (Sigma-Aldrich) or for EEA1 staining 0.01% Triton-X100 (Sigma-Aldrich). The following
749 primary rabbit anti-human antibodies were used to label intracellular compartments: calreticulin for
750 the ER (Sigma-Aldrich), GM130 for the Golgi apparatus (Cell Signalling Technology), EEA1 for early
751 endosomes (ThermoFisher) and LAMP1 for late endosomes/lysosomes (Abcam). This was followed by
752 Donkey anti-Rabbit IgG conjugated to Alexa Fluor™ 546 (ThermoFisher) and DAPI nuclear staining
753 (Sigma-Aldrich). Cells were washed several times between each staining step and then covered in
754 degassed imaging buffer (5% (v/v) Glycerol, 2.5% (w/v) DABCO Powder in PBS, pH 8.5). GFP was used
755 to identify the location and signal strength of the MR1-GFP construct. Two biological repeats were
756 completed for each set of assay conditions.

757 Cells were imaged using the Opera Phenix™ Plus (Perkin Elmer) with the 40X water objective, under
758 control of the Harmony software. A minimum of 4 fields of view (FOV) were imaged per well, with five
759 planes, each 0.5 µm apart, acquired in each channel. Maximum Z-stack projections were created for
760 each FOV and flat field correction was applied through ImageJ FIJI software.¹¹⁶ A segmentation map
761 of the cells within each FOV defining the subcellular compartments was created with ilastik software.⁸²
762 After normalising the median MR1-GFP FOV signal to the control samples within the corresponding
763 experimental condition, the median MR1-GFP signal at each subcellular location was calculated with
764 ImageJ by overlaying the segmentation map. Fold change in the median MR1-GFP signal in the FOV at
765 each subcellular compartment in infected cells compared to corresponding mock infected or RAd-Ctrl
766 infected samples was calculated. In addition, the median MR1-GFP signal within each FOV was used
767 to calculate the relative strength of GFP signal restricted to the subcellular compartment compared
768 to the median cell signal. Statistical significance was evaluated with a minimum of 14 FOV.

769 **QUANTIFICATION AND STATISTICAL ANALYSIS**

770 Paired Student's t tests, Welch's unpaired t-test, or ANOVA analyses were performed, as indicated in
771 each figure legend, using GraphPad Prism software (LLC). Data are presented as dot plots (flow
772 cytometry and RT-qPCR) with the mean +/- SEM, or violin plots (fluorescence microscopy) with the
773 median and quartiles. Statistical significance is represented as * p<0.05, ** p<0.005, *** p<0.0005, or ****
774 p<0.0001. Number of experimental repeats (flow cytometry, RT-qPCR and fluorescence microscopy) and
775 independent FOV (fluorescence microscopy) are indicated in each figure legend.

776 Supplemental Information Titles and Legends

777 **Figure S1. Staining of subcellular compartments is consistent in Mock, HSV-1 and HSV-2 infected**
 778 **cells at 6 h p.i., Related to Figure 8.** ARPE-19 MR1-GFP cells were infected (MOI 5) with HSV-2 (strain
 779 186), HSV-1 strains 17syn+ or 17(41-) lacking expression of vhs or mock infected in parallel. Cells were
 780 treated with Ac-6-FP (5 μ M) for 16 h prior to infection. Cells were stained at 6 h p.i. with wheat germ
 781 agglutinin (WGA) (plasma membrane) and then permeabilised and stained for calreticulin (ER), GM130
 782 (Golgi Apparatus), EEA1 (early endosomes) or LAMP1 (Late endosomes/lysosomes) and DAPI
 783 (nucleus). Representative images from at least 14 fields of view in two independent experiments
 784 acquired with Opera Phenix Plus and Harmony software. Scale bar 50 μ m.

785

786 References

- 787 1. Dusseaux, M., Martin, E., Serriari, N., Peguillet, I., Premel, V., Louis, D., Milder, M., Le
 788 Bourhis, L., Soudais, C., Treiner, E., and Lantz, O. (2011). Human MAIT cells are xenobiotic-
 789 resistant, tissue-targeted, CD161(hi) IL-17-secreting T cells. *Blood* *117*, 1250-1259.
 790 10.1182/blood-2010-08-303339.
- 791 2. Gibbs, A., Leeansyah, E., Introini, A., Paquin-Proulx, D., Hasselrot, K., Andersson, E., Broliden,
 792 K., Sandberg, J.K., and Tjernlund, A. (2017). MAIT cells reside in the female genital mucosa
 793 and are biased towards IL-17 and IL-22 production in response to bacterial stimulation.
 794 *Mucosal Immunology* *10*, 35-45. 10.1038/mi.2016.30.
- 795 3. Tang, X.Z., Jo, J., Tan, A.T., Sandalova, E., Chia, A., Tan, K.C., Lee, K.H., Gehring, A.J., De
 796 Libero, G., and Bertolotti, A. (2013). IL-7 Licenses Activation of Human Liver Intrahepatic
 797 Mucosal-Associated Invariant T Cells. *Journal of Immunology* *190*, 3142-3152.
 798 10.4049/jimmunol.1203218.
- 799 4. Constantinides, M.G., Linehan, J.L., Sen, S., Shaik, J., Roy, S., LeGrand, J.L., Bouladoux, N.,
 800 Adams, E.J., and Belkaid, Y. (2017). Mucosal-associated invariant T cells respond to
 801 cutaneous microbiota. *Journal of Immunology* *198*.
- 802 5. Leeansyah, E., Svard, J., Dias, J., Buggert, M., Nystrom, J., Quigley, M.F., Moll, M.,
 803 Sonnerborg, A., Nowak, P., and Sandberg, J.K. (2015). Arming of MAIT Cell Cytolytic
 804 Antimicrobial Activity Is Induced by IL-7 and Defective in HIV-1 Infection. *PLOS Pathogens* *11*,
 805 e1005072. 10.1371/journal.ppat.1005072.
- 806 6. Porcelli, S., Yockey, C.E., Brenner, M.B., and Balk, S.P. (1993). Analysis of T-cell antigen
 807 receptor (TCR) expression by human peripheral blood CD4-8-alpha/beta T-cells
 808 demonstrates preferential use of several V-beta genes and an invariant TCR alpha-chain.
 809 *Journal of Experimental Medicine* *178*, 1-16. 10.1084/jem.178.1.1.
- 810 7. Tilloy, F., Treiner, E., Park, S.H., Garcia, C., Lemonnier, F., de la Salle, H., Bendelac, A.,
 811 Bonneville, M., and Lantz, O. (1999). An invariant T cell receptor alpha chain defines a novel
 812 TAP-independent major histocompatibility complex class Ib-restricted alpha/beta T cell

- 813 subpopulation in mammals. *Journal of Experimental Medicine* 189, 1907-1921.
814 10.1084/jem.189.12.1907.
- 815 8. Reantragoon, R., Corbett, A.J., Sakala, I.G., Gherardin, N.A., Furness, J.B., Chen, Z.J., Eckle,
816 S.B.G., Uldrich, A.P., Birkinshaw, R.W., Patel, O., et al. (2013). Antigen-loaded MR1 tetramers
817 define T cell receptor heterogeneity in mucosal-associated invariant T cells. *Journal of*
818 *Experimental Medicine* 210, 2305-2320. 10.1084/jem.20130958.
- 819 9. van Wilgenburg, B., Loh, L., Chen, Z.J., Pediongco, T.J., Wang, H.M., Shi, M., Zhao, Z.,
820 Koutsakos, M., Nussing, S., Sant, S., et al. (2018). MAIT cells contribute to protection against
821 lethal influenza infection in vivo. *Nature Communications* 9, 9, 4706. 10.1038/s41467-018-
822 07207-9.
- 823 10. Loh, L., Wang, Z.F., Sant, S., Koutsakos, M., Jegaskanda, S., Corbett, A.J., Liu, L.G., Fairlie,
824 D.P., Crowe, J., Rossjohn, J., et al. (2016). Human mucosal-associated invariant T cells
825 contribute to antiviral influenza immunity via IL-18-dependent activation. *Proceedings of the*
826 *National Academy of Sciences of the United States of America* 113, 10133-10138.
827 10.1073/pnas.1610750113.
- 828 11. Kjer-Nielsen, L., Patel, O., Corbett, A.J., Le Nours, J., Meehan, B., Liu, L.G., Bhati, M., Chen,
829 Z.J., Kostenko, L., Reantragoon, R., et al. (2012). MR1 presents microbial vitamin B
830 metabolites to MAIT cells. *Nature* 491, 717-723. 10.1038/nature11605.
- 831 12. van Wilgenburg, B., Scherwitzl, I., Hutchinson, E.C., Leng, T.Q., Kurioka, A., Kulicke, C., de
832 Lara, C., Cole, S., Vasanawathana, S., Limpitikul, W., et al. (2016). MAIT cells are activated
833 during human viral infections. *Nature Communications* 7, 11653. 10.1038/ncomms11653.
- 834 13. Phetsouphanh, C., Phalora, P., Hackstein, C.P., Thornhill, J., Munier, C.M.L., Meyerowitz, J.,
835 Murray, L., VanVuuren, C., Goedhals, D., Drexhage, L., et al. (2021). Human MAIT cells
836 respond to and suppress HIV-1. *Elife* 10. 10.7554/eLife.50324.
- 837 14. Lal, K.G., Kim, D., Costanzo, M.C., Creegan, M., Leeansyah, E., Dias, J., Paquin-Proulx, D.,
838 Eller, L.A., Schuetz, A., Phuang-Ngern, Y., et al. (2020). Dynamic MAIT cell response with
839 progressively enhanced innateness during acute HIV-1 infection. *Nature Communications* 11,
840 272. 10.1038/s41467-019-13975-9.
- 841 15. Paquin-Proulx, D., Greenspun, B.C., Costa, E.A.S., Segurado, A.C., Kallas, E.G., Nixon, D.F.,
842 and Leal, F.E. (2017). MAIT cells are reduced in frequency and functionally impaired in
843 human T lymphotropic virus type 1 infection: Potential clinical implications. *PloS one* 12,
844 e0175345. 10.1371/journal.pone.0175345.
- 845 16. Yong, Y.K., Saeidi, A., Tan, H.Y., Rosmawati, M., Enstrom, P.F., Al Batran, R., Vasuki, V.,
846 Chattopadhyay, I., Murugesan, A., Vignesh, R., et al. (2018). Hyper-Expression of PD-1 Is
847 Associated with the Levels of Exhausted and Dysfunctional Phenotypes of Circulating
848 CD161(++)TCR iV alpha 7.2(+) Mucosal-Associated Invariant T Cells in Chronic Hepatitis B
849 Virus Infection. *Front. immunol.* 9, 472. 10.3389/fimmu.2018.00472.
- 850 17. Yong, Y.K., Tan, H.Y., Saeidi, A., Rosmawati, M., Atiya, N., Ansari, A.W., Rajarajeswaran, J.,
851 Vadivelu, J., Velu, V., Larsson, M., and Shankar, E.M. (2017). Decrease of CD69 levels on TCR
852 Vα7.2(+)CD4(+) innate-like lymphocytes is associated with impaired cytotoxic functions in
853 chronic hepatitis B virus-infected patients. *Innate Immun* 23, 459-467.
854 10.1177/1753425917714854.

- 855 18. Dias, J., Hengst, J., Parrot, T., Leeansyah, E., Lunemann, S., Malone, D.F.G., Hardtke, S.,
856 Strauss, O., Zimmer, C.L., Berglin, L., et al. (2019). Chronic hepatitis delta virus infection leads
857 to functional impairment and severe loss of MAIT cells. *Journal of Hepatology* 71, 301-312.
858 10.1016/j.jhep.2019.04.009.
- 859 19. Huang, W.Y., He, W.J., and Gao, Y.F. (2020). Mucosal-associated invariant T-cells are severely
860 reduced and exhausted in humans with chronic HBV infection. *Journal of viral hepatitis* 27,
861 1096-1107. 10.1111/jvh.13341.
- 862 20. Beudeker, B.J.B., van Oord, G.W., Arends, J.E., zur Wiesch, J.S., van der Heide, M.S., de
863 Knecht, R.J., Verbon, A., Boonstra, A., and Claassen, M.A.A. (2018). Mucosal-associated
864 invariant T-cell frequency and function in blood and liver of HCV mono- and HCV/HIV co-
865 infected patients with advanced fibrosis. *Liver International* 38, 458-468. 10.1111/liv.13544.
- 866 21. Bolte, F.J., O'Keefe, A.C., Webb, L.M., Serti, E., Rivera, E., Liang, T.J., Ghany, M., and
867 Rehmann, B. (2017). Intra-Hepatic Depletion of Mucosal-Associated Invariant T Cells in
868 Hepatitis C Virus-Induced Liver Inflammation. *Gastroenterology* 153, 1392-1403.
869 10.1053/j.gastro.2017.07.043.
- 870 22. Leeansyah, E., Ganesh, A., Quigley, M.F., Sonnerborg, A., Andersson, J., Hunt, P.W.,
871 Somsouk, M., Deeks, S.G., Martin, J.N., Moll, M., et al. (2013). Activation, exhaustion, and
872 persistent decline of the antimicrobial MR1-restricted MAIT-cell population in chronic HIV-1
873 infection. *Blood* 121, 1124-1135. 10.1182/blood-2012-07-445429.
- 874 23. Wong, E.B., Akilimali, N.A., Govender, P., Sullivan, Z.A., Cosgrove, C., Pillay, M., Lewinsohn,
875 D.M., Bishai, W.R., Walker, B.D., Ndung'u, T., et al. (2013). Low Levels of Peripheral
876 CD161++CD8+Mucosal Associated Invariant T (MAIT) Cells Are Found in HIV and HIV/TB Co-
877 Infection. *PloS one* 8, e83474. 10.1371/journal.pone.0083474.
- 878 24. Saeidi, A., Tien, V.L.T., Al-Batran, R., Al-Darraj, H.A., Tan, H.Y., Yong, Y.K., Ponnampalavanar,
879 S., Barathan, M., Rukumani, D.V., Ansari, A.W., et al. (2015). Attrition of TCR Va7.2+CD161++
880 MAIT Cells in HIV-Tuberculosis Co-Infection Is Associated with Elevated Levels of PD-1
881 Expression. *PloS one* 10, e0124659. 10.1371/journal.pone.0124659.
- 882 25. Freeman, M.L., Morris, S.R., and Lederman, M.M. (2017). CD161 Expression on Mucosa-
883 Associated Invariant T Cells is Reduced in HIV-Infected Subjects Undergoing Antiretroviral
884 Therapy Who Do Not Recover CD4+ T Cells. *Pathogens & immunity* 2, 335-351.
885 10.20411/pai.v2i3.136.
- 886 26. Jouan, Y., Guillon, A., Gonzalez, L., Perez, Y., Boisseau, C., Ehrmann, S., Ferreira, M., Daix, T.,
887 Jeannet, R., François, B., et al. (2020). Phenotypical and functional alteration of
888 unconventional T cells in severe COVID-19 patients. *J Exp Med* 217. 10.1084/jem.20200872.
- 889 27. Youngs, J., Provine, N.M., Lim, N., Sharpe, H.R., Amini, A., Chen, Y.-L., Luo, J., Edmans, M.D.,
890 Zacharopoulou, P., Chen, W., et al. (2021). Identification of immune correlates of fatal
891 outcomes in critically ill COVID-19 patients. *PLOS Pathogens* 17, e1009804-e1009804.
892 10.1371/journal.ppat.1009804.
- 893 28. Lu, B., Liu, M., Wang, J., Fan, H., Yang, D., Zhang, L., Gu, X., Nie, J., Chen, Z., Corbett, A.J., et
894 al. (2020). IL-17 production by tissue-resident MAIT cells is locally induced in children with
895 pneumonia. *Mucosal Immunology*. 10.1038/s41385-020-0273-y.

- 896 29. Sobkowiak, M.J., Davanian, H., Heymann, R., Gibbs, A., Emgard, J., Dias, J., Aleman, S.,
897 Kruger-Weiner, C., Moll, M., Tjernlund, A., et al. (2019). Tissue-resident MAIT cell
898 populations in human oral mucosa exhibit an activated profile and produce IL-17. *European*
899 *Journal of Immunology* *49*, 133-143. 10.1002/eji.201847759.
- 900 30. Slichter, C.K., McDavid, A., Miller, H.W., Finak, G., Seymour, B.J., McNevin, J.P., Diaz, G.,
901 Czartoski, J.L., McElrath, M.J., Gottardo, R., and Prlic, M. (2016). Distinct activation
902 thresholds of human conventional and innate-like memory T cells. *JCI Insight* *1*.
903 10.1172/jci.insight.86292.
- 904 31. Chen, Z., Wang, H., D'Souza, C., Sun, S., Kostenko, L., Eckle, S.B.G., Meehan, B.S., Jackson,
905 D.C., Strugnell, R.A., Cao, H., et al. (2017). Mucosal-associated invariant T-cell activation and
906 accumulation after in vivo infection depends on microbial riboflavin synthesis and co-
907 stimulatory signals. *Mucosal Immunology* *10*, 58-68. 10.1038/mi.2016.39.
- 908 32. Hinks, T.S.C., Marchi, E., Jabeen, M., Olshansky, M., Kurioka, A., Pediongco, T.J., Meehan,
909 B.S., Kostenko, L., Turner, S.J., Corbett, A.J., et al. (2019). Activation and In Vivo Evolution of
910 the MAIT Cell Transcriptome in Mice and Humans Reveals Tissue Repair Functionality. *Cell*
911 *Reports* *28*, 3249-3262.e3245. 10.1016/j.celrep.2019.07.039.
- 912 33. Samer, C., Traves, R., Purohit, S.K., Abendroth, A., McWilliam, H.E.G., and Slobedman, B.
913 (2021). Viral Impacts on MR1 Antigen Presentation to MAIT Cells. *Critical Reviews in*
914 *Immunology* *41*, 49-67. 10.1615/CritRevImmUnol.2022041981.
- 915 34. Li, Y., Shi, C.W., Zhang, Y.T., Huang, H.B., Jiang, Y.L., Wang, J.Z., Cao, X., Wang, N., Zeng, Y.,
916 Yang, G.L., et al. (2022). Riboflavin Attenuates Influenza Virus Through Cytokine-Mediated
917 Effects on the Diversity of the Gut Microbiota in MAIT Cell Deficiency Mice. *Front Microbiol*
918 *13*, 916580. 10.3389/fmicb.2022.916580.
- 919 35. Eberle, R.J., Olivier, D.S., Amaral, M.S., Pacca, C.C., Nogueira, M.L., Arni, R.K., Willbold, D.,
920 and Coronado, M.A. (2022). Riboflavin, a Potent Neuroprotective Vitamin: Focus on
921 Flavivirus and Alphavirus Proteases. *Microorganisms* *10*. 10.3390/microorganisms10071331.
- 922 36. Chancellor, A., Simmons, R.A., Khanolkar, R.C., Nosi, V., Beshirova, A., Berloffo, G., Colombo,
923 R., Karuppiyah, V., Pentier, J.M., Tubb, V., et al. (2023). Promiscuous recognition of MR1
924 drives self-reactive mucosal-associated invariant T cell responses. *Journal of Experimental*
925 *Medicine* *220*, 25, e20221939. 10.1084/jem.20221939.
- 926 37. McSharry, B.P., Samer, C., McWilliam, H.E.G., Ashley, C.L., Yee, M.B., Steain, M., Liu, L.G.,
927 Fairlie, D.P., Kinchington, P.R., McCluskey, J., et al. (2020). Virus-Mediated Suppression of
928 the Antigen Presentation Molecule MR1. *Cell Reports* *30*, 2948-+.
929 10.1016/j.celrep.2020.02.017.
- 930 38. Purohit, S.K., Samer, C., McWilliam, H.E.G., Traves, R., Steain, M., McSharry, B.P.,
931 Kinchington, P.R., Tscharke, D.C., Villadangos, J.A., Rossjohn, J., et al. (2021). Varicella zoster
932 virus impairs expression of the non-classical major histocompatibility complex class I-related
933 gene protein (MR1). *The Journal of Infectious Diseases* *227*, 391-401. 10.1093/infdis/jiab526.
- 934 39. Ashley, C.L., McSharry, B.P., McWilliam, H.E.G., Stanton, R.J., Fielding, C.A., Mathias, R.A.,
935 Fairlie, D.P., McCluskey, J., Villadangos, J.A., Rossjohn, J., et al. (2023). Suppression of MR1
936 by human cytomegalovirus inhibits MAIT cell activation. *Front. immunol.* *14*.
937 10.3389/fimmu.2023.1107497.

- 938 40. Roizman, B., Knipe, D.M., and Whitely, R.J. (2013). Herpes Simplex Viruses. In D.M. Knipe,
939 and P.M. Howley, eds. *Fields Virology*. 6 ed. Wolters Kluwer Health/Lippincott Williams &
940 Wilkins.
- 941 41. Hill, A., Jugovic, P., York, I., Russ, G., Bennink, J., Yewdell, J., Ploegh, H., and Johnson, D.
942 (1995). Herpes-Simplex Virus Turns off the TAP to evade Host Immunity. *Nature* 375, 411-
943 415. 10.1038/375411a0.
- 944 42. van Lint, A.L., Murawski, M.R., Goodbody, R.E., Severa, M., Fitzgerald, K.A., Finberg, R.W.,
945 Knipe, D.M., and Kurt-Jones, E.A. (2010). Herpes Simplex Virus Immediate-Early ICPO Protein
946 Inhibits Toll-Like Receptor 2-Dependent Inflammatory Responses and NF-kappa B Signaling.
947 *J. Virol* 84, 10802-10811. 10.1128/jvi.00063-10.
- 948 43. Wagner, L.M., Bayer, A., and DeLuca, N.A. (2013). Requirement of the N-Terminal Activation
949 Domain of Herpes Simplex Virus ICP4 for Viral Gene Expression. *J. Virol* 87, 1010-1018.
950 10.1128/JVI.02844-12.
- 951 44. Neumann, L., Kraas, W., Uebel, S., Jung, G., and Tampe, R. (1997). The active domain of the
952 herpes simplex virus protein ICP47: A potent inhibitor of the transporter associated with
953 antigen processing (TAP). *Journal of Molecular Biology* 272, 484-492.
954 10.1006/jmbi.1997.1282.
- 955 45. Oldham, M.L., Hite, R.K., Steffen, A.M., Damko, E., Li, Z., Walz, T., and Chen, J. (2016). A
956 mechanism of viral immune evasion revealed by cryo-EM analysis of the TAP transporter.
957 *Nature* 529, 537-540. 10.1038/nature16506.
- 958 46. Blees, A., Janulienė, D., Hofmann, T., Koller, N., Schmidt, C., Trowitzsch, S., Moeller, A., and
959 Tampé, R. (2017). Structure of the human MHC-I peptide-loading complex. *Nature* 551, 525-
960 528. 10.1038/nature24627.
- 961 47. McWilliam, H.E.G., Mak, J.Y.W., Awad, W., Zorkau, M., Cruz-Gomez, S., Lim, H.J., Yan, Y.,
962 Wormald, S., Dagley, L.F., Eckle, S.B.G., et al. (2020). Endoplasmic reticulum chaperones
963 stabilize ligand-receptive MR1 molecules for efficient presentation of metabolite antigens.
964 *Proceedings of the National Academy of Sciences*, 202011260. 10.1073/pnas.2011260117.
- 965 48. Velusamy, T., Singh, N., Croft, S., Smith, S., and Tschärke, D.C. (2023). The expression and
966 function of HSV ICP47 and its promoter in mice. *J. Virol*, e0110723-e0110723.
967 10.1128/jvi.01107-23.
- 968 49. Hill, A.B., Barnett, B.C., McMichael, A.J., and McGeoch, D.J. (1994). HLA class I molecules are
969 not transported to the cell surface in cells infected with herpes simplex virus types 1 and 2.
970 *The Journal of immunology* (1950) 152, 2736-2741. 10.4049/jimmunol.152.6.2736.
- 971 50. York, I.A., Roop, C., Andrews, D.W., Riddell, S.R., Graham, F.L., and Johnson, D.C. (1994). A
972 cytosolic herpes-simplex virus protein inhibits antigen presentation to CD8(+) T-
973 lymphocytes. *Cell* 77, 525-535. 10.1016/0092-8674(94)90215-1.
- 974 51. McWilliam, H.E.G., Eckle, S.B.G., Theodossis, A., Liu, L.G., Chen, Z.J., Wubben, J.M., Fairlie,
975 D.P., Strugnell, R.A., Mintern, J.D., McCluskey, J., et al. (2016). The intracellular pathway for
976 the presentation of vitamin B-related antigens by the antigen-presenting molecule MR1.
977 *Nature Immunology* 17, 531-537. 10.1038/ni.3416.

- 978 52. Teo, C.S.H., and O'Hare, P. (2018). A bimodal switch in global protein translation coupled to
979 eIF4H relocalisation during advancing cell-cell transmission of herpes simplex virus. *PLOS*
980 *Pathogens* 14, 30, e1007196. 10.1371/journal.ppat.1007196.
- 981 53. Elliott, G., and O'Hare, P. (1999). Live-cell analysis of a green fluorescent protein-tagged
982 herpes simplex virus infection. *J. Virol* 73, 4110-4119.
- 983 54. Fox, H.L., Dembowski, J.A., and DeLuca, N.A. (2017). A Herpesviral Immediate Early Protein
984 Promotes Transcription Elongation of Viral Transcripts. *Mbio* 8, 16, e00745-17.
985 10.1128/mBio.00745-17.
- 986 55. Bastian, T.W., Livingston, C.M., Weller, S.K., and Rice, S.A. (2010). Herpes Simplex Virus Type
987 1 Immediate-Early Protein ICP22 Is Required for VICE Domain Formation during Productive
988 Viral Infection. *J. Virol* 84, 2384. 10.1128/JVI.01686-09.
- 989 56. Burch, A.D., and Weller, S.K. (2004). Nuclear sequestration of cellular chaperone and
990 proteasomal machinery during herpes simplex virus type 1 infection. *J. Virol* 78, 7175-7185.
991 10.1128/JVI.78.13.7175-7185.2004.
- 992 57. Adlakha, M., Livingston, C.M., Bezsonova, I., and Weller, S.K. (2020). The Herpes Simplex
993 Virus 1 Immediate Early Protein ICP22 Is a Functional Mimic of a Cellular J Protein. *J. Virol* 94,
994 01564-01519. 10.1128/jvi.01564-19.
- 995 58. Bastian, T.W., and Rice, S.A. (2009). Identification of sequences in herpes simplex virus type
996 1 ICP22 that influence RNA polymerase II modification and viral late gene expression. *J. Virol*
997 83, 128-139. 10.1128/jvi.01954-08.
- 998 59. Guo, L., Wu, W.-j., Liu, L.-d., Wang, L.-c., Zhang, Y., Wu, L.-q., Guan, Y., and Li, Q.-h. (2012).
999 Herpes Simplex Virus 1 ICP22 Inhibits the Transcription of Viral Gene Promoters by Binding
1000 to and Blocking the Recruitment of P-TEFb. *PLoS one* 7, e45749-e45749.
1001 10.1371/journal.pone.0045749.
- 1002 60. Zaborowska, J., Baumli, S., Laitem, C., O'Reilly, D., Thomas, P.H., O'Hare, P., and Murphy, S.
1003 (2014). Herpes Simplex Virus 1 (HSV-1) ICP22 Protein Directly Interacts with Cyclin-
1004 Dependent Kinase (CDK) 9 to Inhibit RNA Polymerase II Transcription Elongation. *PLoS one* 9,
1005 9, e107654. 10.1371/journal.pone.0107654.
- 1006 61. Fraser, K.A., and Rice, S.A. (2007). Herpes simplex virus immediate-early protein ICP22
1007 triggers loss of serine 2-phosphorylated RNA polymerase II. *J. Virol* 81, 5091-5101.
1008 10.1128/jvi.00184-07.
- 1009 62. Advani, S.J., Brandimarti, R., Weichselbaum, R.R., and Roizman, B. (2000). The disappearance
1010 of cyclins A and B and the increase in activity of the G2/M-phase cellular kinase cdc2 in
1011 herpes simplex virus 1-infected cells require expression of the α 22/U(S)1.5 and U(L)13 viral
1012 genes. *J. Virol* 74, 8-15. 10.1128/JVI.74.1.8-15.2000.
- 1013 63. Orlando, J.S., Astor, T.L., Rundle, S.A., and Schaffer, P.A. (2006). The Products of the Herpes
1014 Simplex Virus Type 1 Immediate-Early US1/US1.5 Genes Downregulate Levels of S-Phase-
1015 Specific Cyclins and Facilitate Virus Replication in S-Phase Vero Cells. *J. Virol* 80, 4005-4016.
1016 10.1128/JVI.80.8.4005-4016.2006.
- 1017 64. Zhang, M., Fu, M., Li, M., Hu, H., Gong, S., and Hu, Q. (2020). Herpes Simplex Virus Type 2
1018 Inhibits Type I IFN Signaling Mediated by the Novel E3 Ubiquitin Protein Ligase Activity of

- 1019 Viral Protein ICP22. *The Journal of immunology* (1950) *205*, 1281-1292.
1020 10.4049/jimmunol.2000418.
- 1021 65. Carter, K.L., and Roizman, B. (1996). The promoter and transcriptional unit of a novel herpes
1022 simplex virus 1 alpha gene are contained in, and encode a protein in frame with, the open
1023 reading frame of the alpha 22 gene. *J. Virol* *70*, 172-178. 10.1128/JVI.70.1.172-178.1996.
- 1024 66. Hagglund, R., Munger, J., Poon, A.P.W., and Roizman, B. (2002). US3 Protein Kinase of
1025 Herpes Simplex Virus 1 Blocks Caspase 3 Activation Induced by the Products of US1.5 and
1026 UL13 Genes and Modulates Expression of Transduced US1.5 Open Reading Frame in a Cell
1027 Type-Specific Manner. *J. Virol* *76*, 743-754. 10.1128/jvi.76.2.743-754.2002.
- 1028 67. Stanton, R.J., McSharry, B.P., Armstrong, M., Tomasec, P., and Wilkinson, G.W.G. (2008). Re-
1029 engineering adenovirus vector systems to enable high-throughput analyses of gene function.
1030 *BioTechniques* *45*, 659-668. 10.2144/000112993.
- 1031 68. Abos, B., del Moral, M.G., Gozalbo-Lopez, B., Lopez-Relano, J., Viana, V., and Martinez-
1032 Naves, E. (2011). Human MR1 expression on the cell surface is acid sensitive, proteasome
1033 independent and increases after culturing at 26 degrees C. *Biochem. Biophys. Res. Commun.*
1034 *411*, 632-636. 10.1016/j.bbrc.2011.07.007.
- 1035 69. Everly, D.N., Feng, P.H., Mian, I.S., and Read, G.S. (2002). mRNA degradation by the virion
1036 host shutoff (Vhs) protein of herpes simplex virus: Genetic and biochemical evidence that
1037 Vhs is a nuclease. *J. Virol* *76*, 8560-8571. 10.1128/jvi.76.17.8560-8571.2002.
- 1038 70. Feng, P.H., Everly, D.N., and Read, G.S. (2001). MRNA decay during herpesvirus infections:
1039 Interaction between a putative viral nuclease and a cellular translation factor. *J. Virol* *75*,
1040 10272-10280. 10.1128/jvi.75.21.10272-10280.2001.
- 1041 71. Taddeo, B., and Roizman, B. (2006). The virion host shutoff protein (U(L)41) of herpes
1042 simplex virus 1 is an endoribonuclease with a substrate specificity similar to that of RNase A.
1043 *J. Virol* *80*, 9341-9345. 10.1128/jvi.01008-06.
- 1044 72. Feng, P.H., Everly, D.N., and Read, G.S. (2005). mRNA decay during herpes simplex virus
1045 (HSV) infections: Protein-protein interactions involving the HSV virion host shutoff protein
1046 and translation factors eIF4H and eIF4A. *J. Virol* *79*, 9651-9664. 10.1128/jvi.79.15.9651-
1047 9664.2005.
- 1048 73. Shiflett, L.A., and Read, G.S. (2013). mRNA Decay during Herpes Simplex Virus (HSV)
1049 Infections: Mutations That Affect Translation of an mRNA Influence the Sites at Which It Is
1050 Cleaved by the HSV Virion Host Shutoff (Vhs) Protein. *J. Virol* *87*, 94. 10.1128/JVI.01557-12.
- 1051 74. Riegert, P., Wanner, V., and Bahram, S. (1998). Genomics, isoforms, expression, and
1052 phylogeny of the MHC class I-related MR1 gene. *Journal of Immunology* *161*, 4066-4077.
- 1053 75. Lion, J., Debuysscher, V., Wlodarczyk, A., Hodroge, A., Serriari, N.E., Choteau, L., Ouled-
1054 Haddou, H., Plistat, M., Lassoued, K., Lantz, O., and Treiner, E. (2013). MR1B, a natural
1055 spliced isoform of the MHC-related 1 protein, is expressed as homodimers at the cell surface
1056 and activates MAIT cells. *European Journal of Immunology* *43*, 1363-1373.
1057 10.1002/eji.201242461.
- 1058 76. Narayanan, G.A., Nellore, A., Tran, J., Worley, A.H., Meermeier, E.W., Karamooz, E., Huber,
1059 M.E., Kurapova, R., Tafesse, F.G., Harriff, M.J., and Lewinsohn, D.M. (2020). Alternative

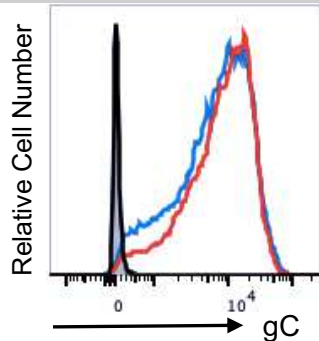
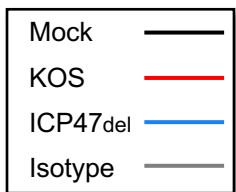
- 1060 splicing of MR1 regulates antigen presentation to MAIT cells. *Scientific Reports* 10, 15429.
1061 10.1038/s41598-020-72394-9.
- 1062 77. Friedel, C.C., Whisnant, A.W., Djakovic, L., Rutkowski, A.J., Friedl, M.-S., Kluge, M.,
1063 Williamson, J.C., Sai, S., Vidal, R.O., Sauer, S., et al. (2021). Dissecting Herpes Simplex Virus 1-
1064 Induced Host Shutoff at the RNA Level. *J. Virol* 95, 01399-01320. 10.1128/JVI.01399-20.
- 1065 78. Hennig, T., Djakovic, L., Dölken, L., and Whisnant, A.W. (2021). A review of the multipronged
1066 attack of herpes simplex virus 1 on the host transcriptional machinery. *Viruses* 13, 1836.
1067 10.3390/v13091836.
- 1068 79. Fenwick, M.L., and Everett, R.D. (1990). Inactivation of the shutoff gene (UL41) of Herpes-
1069 Simplex virus type-1 and type-2. *Journal of General Virology* 71, 2961-2967. 10.1099/0022-
1070 1317-71-12-2961.
- 1071 80. Lim, H.J., Wubben, J.M., Garcia, C.P., Cruz-Gomez, S., Deng, J., Mak, J.Y.W., Hachani, A.,
1072 Anderson, R.J., Painter, G.F., Goyette, J., et al. (2022). A specialized tyrosine-based
1073 endocytosis signal in MR1 controls antigen presentation to MAIT cells. *The Journal of cell*
1074 *biology* 221. 10.1083/jcb.202110125.
- 1075 81. Harriff, M.J., Karamooz, E., Burr, A., Grant, W.F., Canfield, E.T., Sorensen, M.L., Moita, L.F.,
1076 and Lewinsohn, D.M. (2016). Endosomal MR1 Trafficking Plays a Key Role in Presentation of
1077 *Mycobacterium tuberculosis* Ligands to MAIT Cells. *PLOS Pathogens* 12, e1005524,
1078 e1005524. 10.1371/journal.ppat.1005524.
- 1079 82. Berg, S., Kutra, D., Kroeger, T., Straehle, C.N., Kausler, B.X., Haubold, C., Schiegg, M., Ales, J.,
1080 Beier, T., Rudy, M., et al. (2019). ilastik: interactive machine learning for (bio)image analysis.
1081 *Nature Methods* 16, 1226-1232. 10.1038/s41592-019-0582-9.
- 1082 83. Wertheim, J.O., Hostager, R., Ryu, D., Merkel, K., Angedakin, S., Arandjelovic, M., Ayimisin,
1083 E.A., Babweteera, F., Bessone, M., Brun-Jeffery, K.J., et al. (2021). Discovery of Novel Herpes
1084 Simplexviruses in Wild Gorillas, Bonobos, and Chimpanzees Supports Zoonotic Origin of HSV-
1085 2. *Mol. Biol. Evol.* 38, 2818-2830. 10.1093/molbev/msab072.
- 1086 84. Wertheim, J.O., Smith, M.D., Smith, D.M., Scheffler, K., and Pond, S.L.K. (2014). Evolutionary
1087 Origins of Human Herpes Simplex Viruses 1 and 2. *Mol. Biol. Evol.* 31, 2356-2364.
1088 10.1093/molbev/msu185.
- 1089 85. Norberg, P., Tyler, S., Severini, A., Whitley, R., Liljeqvist, J.-Å., and Bergström, T. (2011). A
1090 genome-wide comparative evolutionary analysis of herpes simplex virus type 1 and varicella
1091 zoster virus. *PloS one* 6, e22527-e22527. 10.1371/journal.pone.0022527.
- 1092 86. Scherer, K.M., Manton, J.D., Soh, T.K., Mascheroni, L., Connor, V., Crump, C.M., and
1093 Kaminski, C.F. (2021). A fluorescent reporter system enables spatiotemporal analysis of host
1094 cell modification during herpes simplex virus-1 replication. *The Journal of biological*
1095 *chemistry* 296, 100236-100236. 10.1074/jbc.RA120.016571.
- 1096 87. Johnson, K.E., Chikoti, L., and Chandran, B. (2013). Herpes Simplex Virus 1 Infection Induces
1097 Activation and Subsequent Inhibition of the IFI16 and NLRP3 Inflammasomes. *J. Virol* 87,
1098 5005-5018. 10.1128/jvi.00082-13.

- 1099 88. Orzalli, M.H., Broekema, N.M., and Knipe, D.M. (2016). Relative Contributions of Herpes
1100 Simplex Virus 1 ICP0 and vhs to Loss of Cellular IFI16 Vary in Different Human Cell Types. *J.*
1101 *Virol* *90*, 8351-8359. 10.1128/jvi.00939-16.
- 1102 89. Zhang, J., Wang, K.Z., Wang, S., and Zheng, C.F. (2013). Herpes Simplex Virus 1 E3 Ubiquitin
1103 Ligase ICP0 Protein Inhibits Tumor Necrosis Factor Alpha-Induced NF-kappa B Activation by
1104 Interacting with p65/RelA and p50/NF-kappa B1. *J. Virol* *87*, 12935-12948.
1105 10.1128/jvi.01952-13.
- 1106 90. Huang, S.X., Gilfillan, S., Kim, S., Thompson, B., Wang, X.L., Sant, A.J., Fremont, D.H., Lantz,
1107 O., and Hansen, T.H. (2008). MR1 uses an endocytic pathway to activate mucosal-associated
1108 invariant T cells. *Journal of Experimental Medicine* *205*, 1201-1211. 10.1084/jem.20072579.
- 1109 91. Treiner, E., Duban, L., Bahram, S., Radosavljevic, M., Wanner, V., Tilloy, F., Affaticati, P.,
1110 Gilfillan, S., and Lantz, O. (2003). Selection of evolutionarily conserved mucosal-associated
1111 invariant T cells by MR1. *Nature* *422*, 164-169. 10.1038/nature01433.
- 1112 92. Gold, M.C., Cerri, S., Smyk-Pearson, S., Cansler, M.E., Vogt, T.M., Delepine, J., Winata, E.,
1113 Swarbrick, G.M., Chua, W.J., Yu, Y.Y., et al. (2010). Human mucosal associated invariant T
1114 cells detect bacterially infected cells. *PLoS biology* *8*, e1000407.
1115 10.1371/journal.pbio.1000407.
- 1116 93. Stelz, G., Rucker, E., Rosorius, O., Meyer, G., Stauber, R.H., Spatz, M., Eibl, M.M., and
1117 Hauber, J. (2002). Identification of two nuclear import signals in the alpha-gene product
1118 ICP22 of herpes simplex virus 1. *Virology* *295*, 360-370. 10.1006/viro.2002.1384.
- 1119 94. Poffenberger, K.L., Raichlen, P.E., and Herman, R.C. (1993). In vitro characterization of a
1120 herpes simplex virus type 1 ICP22 deletion mutant. *Virus genes* *7*, 171-186.
1121 10.1007/BF01702397.
- 1122 95. Orlando, J.S., Balliet, J.W., Kushnir, A.S., Astor, T.L., Kosz-Vnenchak, M., Rice, S.A., Knipe,
1123 D.M., and Schaffer, P.A. (2006). ICP22 Is Required for Wild-Type Composition and Infectivity
1124 of Herpes Simplex Virus Type 1 Virions. *J. Virol* *80*, 9381-9390. 10.1128/JVI.01061-06.
- 1125 96. Sears, A.E., Halliburton, I.W., Meignier, B., Silver, S., and Roizman, B. (1985). Herpes simplex
1126 virus 1 mutant deleted in the alpha 22 gene: growth and gene expression in permissive and
1127 restrictive cells and establishment of latency in mice. *J. Virol* *55*, 338-346.
1128 10.1128/JVI.55.2.338-346.1985.
- 1129 97. Suzutani, T., Nagamine, M., Shibaki, T., Ogasawara, M., Yoshida, I., Daikoku, T., Nishiyama,
1130 Y., and Azuma, M. (2000). The role of the UL41 gene of herpes simplex virus type 1 in
1131 evasion of non-specific host defence mechanisms during primary infection. *Journal of*
1132 *General Virology* *81*, 1763-1771. doi.org/10.1099/0022-1317-81-7-1763.
- 1133 98. Pasiaka, T.J., Lu, B., Crosby, S.D., Wylie, K.M., Morrison, L.A., Alexander, D.E., Menachery,
1134 V.D., and Leib, D.A. (2008). Herpes simplex virus virion host shutoff attenuates
1135 establishment of the antiviral state. *J. Virol* *82*, 5527-5535. 10.1128/jvi.02047-07.
- 1136 99. Smith, T.J., Morrison, L.A., and Leib, D.A. (2002). Pathogenesis of herpes simplex virus type 2
1137 virion host shutoff (vhs) mutants. *J. Virol* *76*, 2054-2061. 10.1128/jvi.76.5.2054-2061.2002.

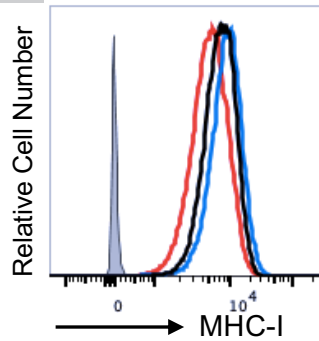
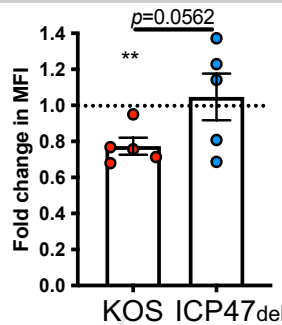
- 1138 100. Korom, M., Wylie, K.M., and Morrison, L.A. (2008). Selective ablation of virion host shutoff
 1139 protein RNase activity attenuates herpes simplex virus 2 in mice. *J. Virol* *82*, 3642-3653.
 1140 10.1128/jvi.02409-07.
- 1141 101. Su, C., and Zheng, C. (2017). Herpes Simplex Virus 1 Abrogates the cGAS/STING-Mediated
 1142 Cytosolic DNA-Sensing Pathway via Its Virion Host Shutoff Protein, UL41. *J. Virol* *91*.
 1143 10.1128/jvi.02414-16.
- 1144 102. Yokota, S., Yokosawa, N., Okabayashi, T., Suzutani, T., Miura, S., Jimbow, K., and Fujii, N.
 1145 (2004). Induction of suppressor of cytokine signaling-3 by herpes simplex virus type 1
 1146 contributes to inhibition of the interferon signaling pathway. *J. Virol* *78*, 6282-6286.
 1147 10.1128/jvi.78.12.6282-6286.2004.
- 1148 103. Shen, G.H., Wang, K.Z., Wang, S., Cai, M.S., Li, M.L., and Zheng, C.F. (2014). Herpes Simplex
 1149 Virus 1 Counteracts Viperin via Its Virion Host Shutoff Protein UL41. *J. Virol* *88*, 12163-12166.
 1150 10.1128/jvi.01380-14.
- 1151 104. Zenner, H.L., Mauricio, R., Banting, G., and Crump, C.M. (2013). Herpes Simplex Virus 1
 1152 Counteracts Tetherin Restriction via Its Virion Host Shutoff Activity. *J. Virol* *87*, 13115-13123.
 1153 10.1128/jvi.02167-13.
- 1154 105. Su, C., Zhang, J., and Zheng, C. (2015). Herpes simplex virus 1 UL41 protein abrogates the
 1155 antiviral activity of hZAP by degrading its mRNA. *Virology journal* *12*, 203-203.
 1156 10.1186/s12985-015-0433-y.
- 1157 106. Samady, L., Costigliola, E., MacCormac, L., McGrath, Y., Cleverley, S., Lilley, C.E., Smith, J.,
 1158 Latchman, D.S., Chain, B., and Coffin, R.S. (2003). Deletion of the virion host shutoff protein
 1159 (vhs) from herpes simplex virus (HSV) relieves the viral block to dendritic cell activation:
 1160 Potential of vhs(-) HSV vectors for dendritic cell-mediated immunotherapy. *J. Virol* *77*, 3768-
 1161 3776. 10.1128/jvi.77.6.3768-3776.2003.
- 1162 107. Tigges, M.A., Leng, S., Johnson, D.C., and Burke, R.L. (1996). Human herpes simplex virus
 1163 (HSV)-specific CD8(+) CTL clones recognize HSV-2-infected fibroblasts after treatment with
 1164 IFN-gamma or when virion host shutoff functions are disabled. *Journal of Immunology* *156*,
 1165 3901-3910.
- 1166 108. Trgovcich, J., Johnson, D., and Roizman, B. (2002). Cell surface major histocompatibility
 1167 complex class II proteins are regulated by the products of the gamma(1)34.5 and U(L)41
 1168 genes of herpes simplex virus 1. *J. Virol* *76*, 6974-6986. 10.1128/jvi.76.14.6974-6986.2002.
- 1169 109. Wang, X., Hennig, T., Whisnant, A.W., Erhard, F., Prusty, B.K., Friedel, C.C., Forouzmand, E.,
 1170 Hu, W., Erber, L., Chen, Y., et al. (2020). Herpes simplex virus blocks host transcription
 1171 termination via the bimodal activities of ICP27. *Nature communications* *11*, 293-293.
 1172 10.1038/s41467-019-14109-x.
- 1173 110. Tormanen, K., Matundan, H.H., Wang, S., Jaggi, U., Mott, K.R., and Ghiasi, H. (2022). Small
 1174 Noncoding RNA (sncRNA1) within the Latency-Associated Transcript Modulates Herpes
 1175 Simplex Virus 1 Virulence and the Host Immune Response during Acute but Not Latent
 1176 Infection. *J. Virol* *96*, e0005422-e0005422. 10.1128/jvi.00054-22.
- 1177 111. Seach, N., Guerri, L., Le Bourhis, L., Mburu, Y., Cui, Y., Bessoles, S., Soudais, C., and Lantz, O.
 1178 (2013). Double Positive Thymocytes Select Mucosal-Associated Invariant T Cells. *Journal of*
 1179 *Immunology* *191*, 6002-6009. 10.4049/jimmunol.1301212.

- 1180 112. Rouxel, O., Da Silva, J., Beaudoin, L., Nel, I., Tard, C., Cagninacci, L., Kïaf, B., Oshima, M.,
1181 Diedisheim, M., Salou, M., et al. (2017). Cytotoxic and regulatory roles of mucosal-associated
1182 invariant T cells in type 1 diabetes. *Nature Immunology* 18, 1321-+. 10.1038/ni.3854.
- 1183 113. Liu, Y., Zhu, P., Wang, W., Tan, X.S., Liu, C.Q., Chen, Y.S., Pei, R.J., Cheng, X., Wu, M., Guo, Q.,
1184 et al. (2021). Mucosal-Associated Invariant T Cell Dysregulation Correlates With Conjugated
1185 Bilirubin Level in Chronic HBV Infection. *Hepatology* 73, 1671-1687. 10.1002/hep.31602.
- 1186 114. Rawls, W.E., Laurel, D., Melnick, J.L., Glicksman, J.M., and Kaufman, R.H. (1968). A search for
1187 viruses in smegma, premalignant and early malignant cervical tissues. The isolation of
1188 herpesviruses with distinct antigenic properties. *American journal of epidemiology* 87, 647-
1189 655. 10.1093/oxfordjournals.aje.a120855.
- 1190 115. Schmittgen, T.D., and Zakrajsek, B.A. (2000). Effect of experimental treatment on
1191 housekeeping gene expression: validation by real-time, quantitative RT-PCR. *Journal of*
1192 *Biochemical and Biophysical Methods* 46, 69-81. doi.org/10.1016/S0165-022X(00)00129-9.
- 1193 116. Schindelin, J., Arganda-Carreras, I., Frise, E., Kaynig, V., Longair, M., Pietzsch, T., Preibisch, S.,
1194 Rueden, C., Saalfeld, S., Schmid, B., et al. (2012). Fiji: an open-source platform for biological-
1195 image analysis. *Nature Methods* 9, 676-682. 10.1038/nmeth.2019.
- 1196

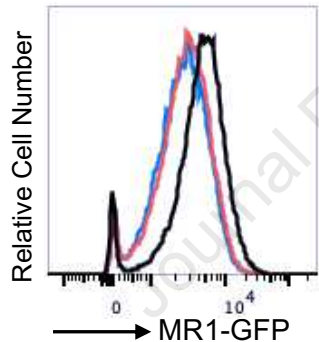
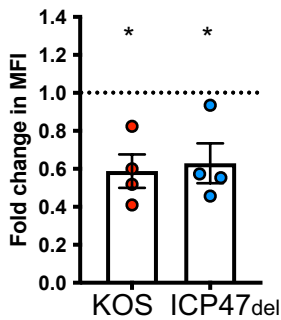
A Surface viral gC



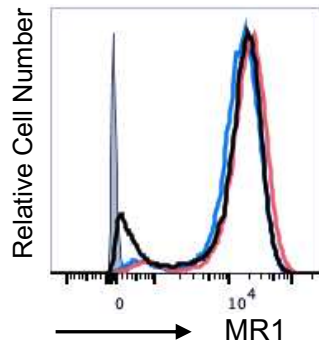
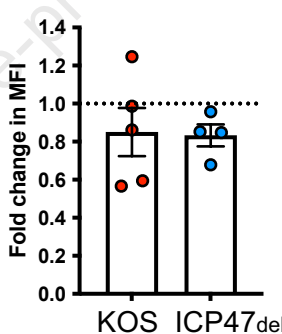
B Surface MHC-I



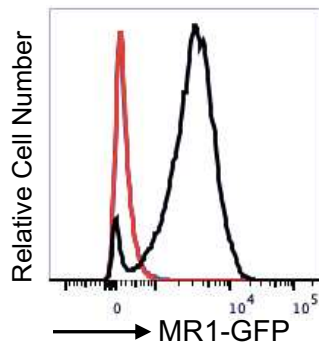
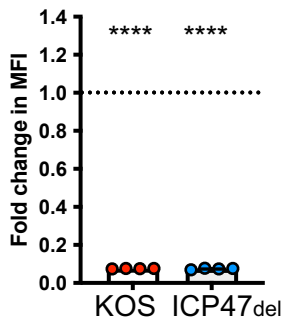
C. Total MR1



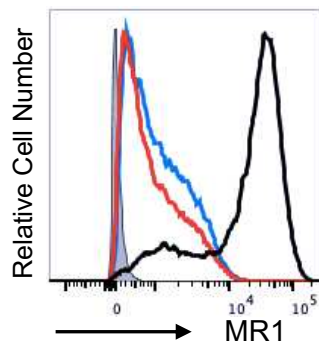
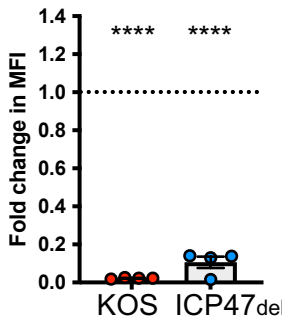
Surface MR1

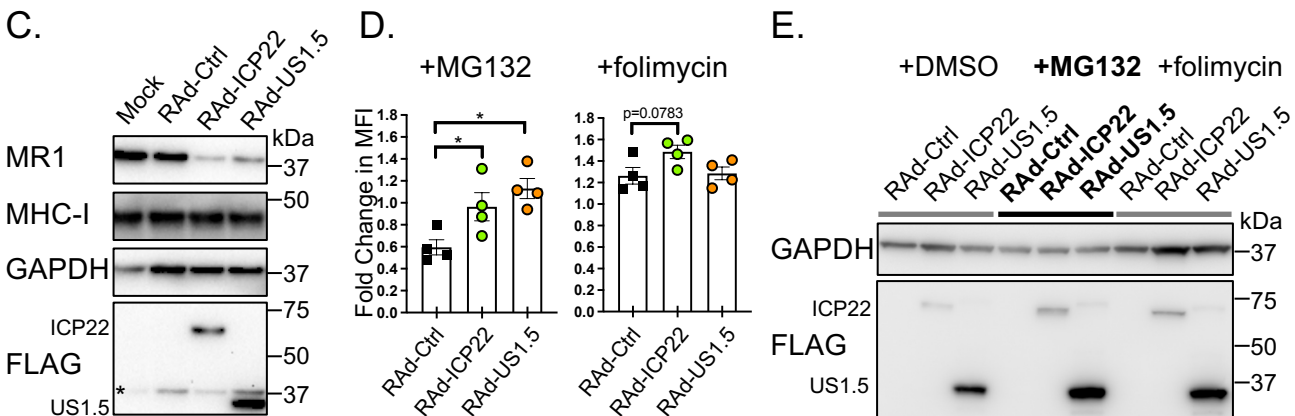
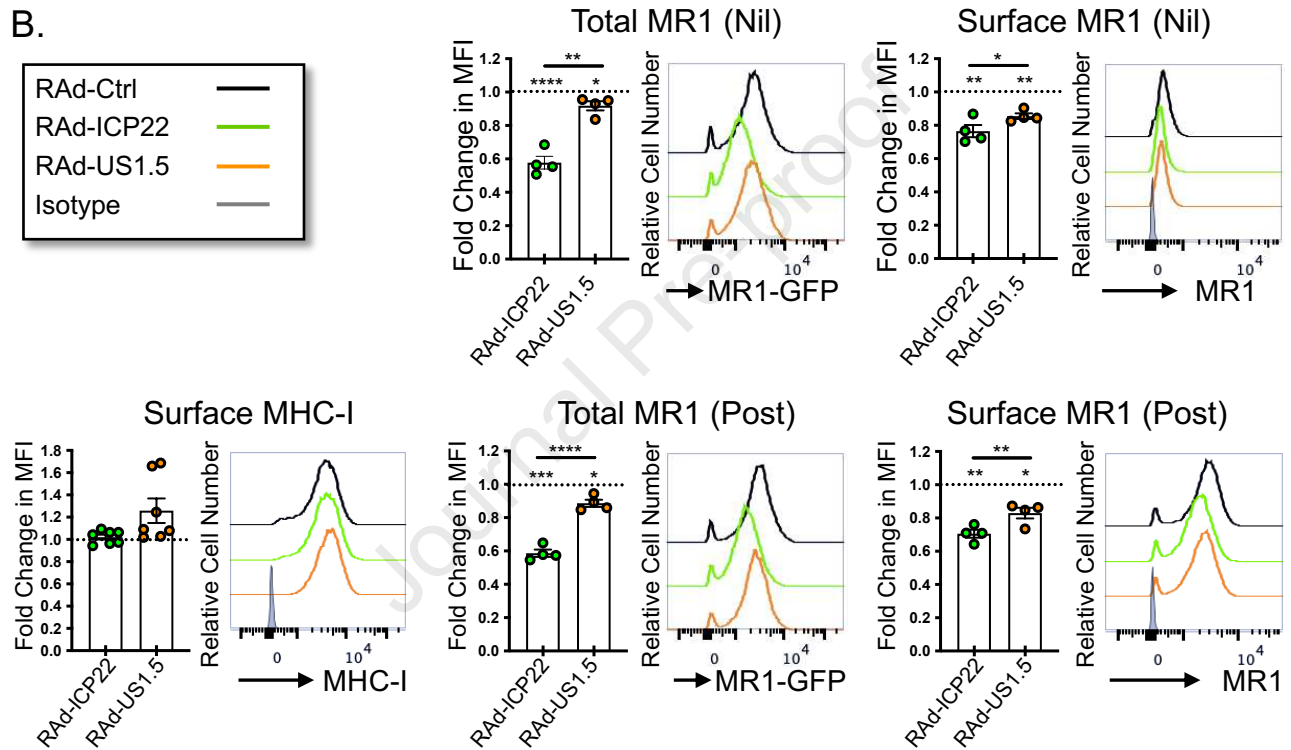
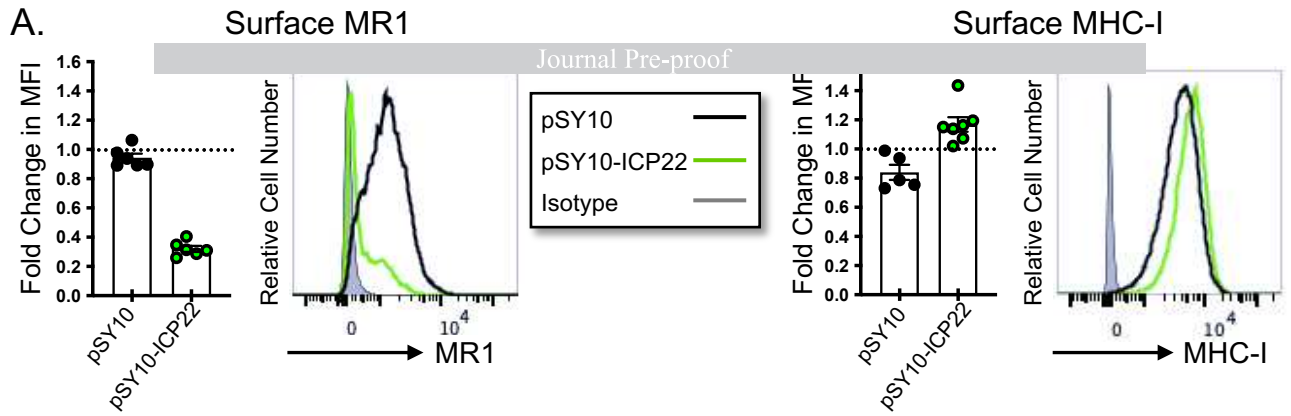


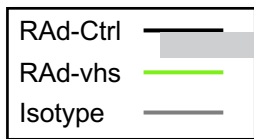
D. Total MR1



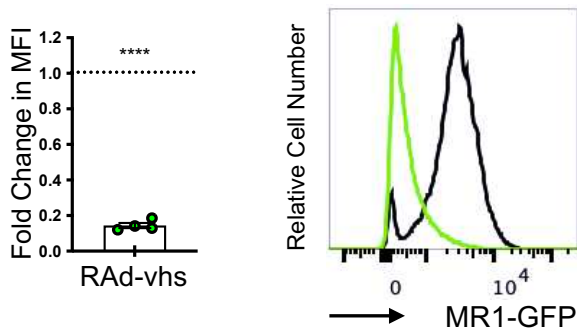
Surface MR1



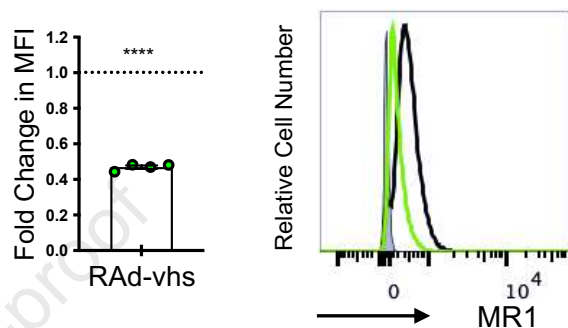




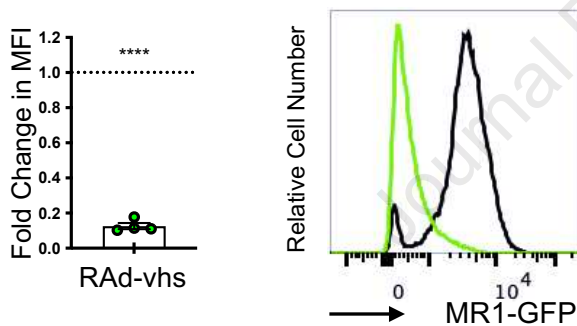
Total MR1 (Nil)



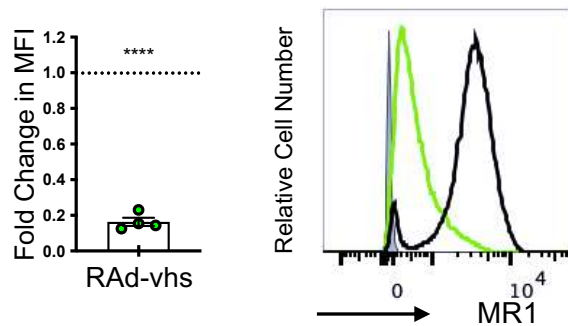
Surface MR1 (Nil)



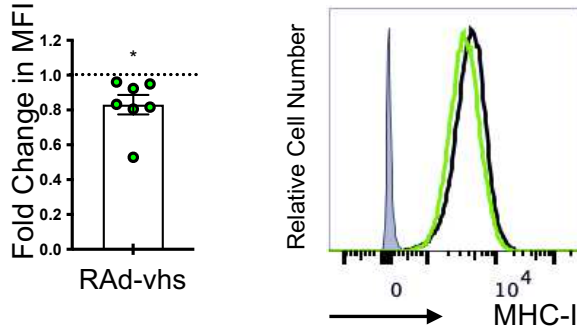
Total MR1 (Post)



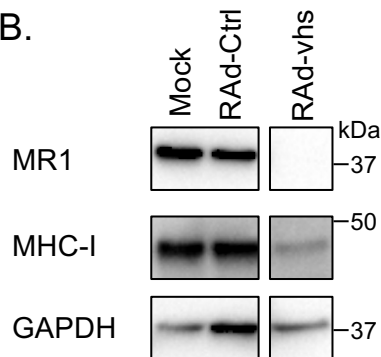
Surface MR1 (Post)



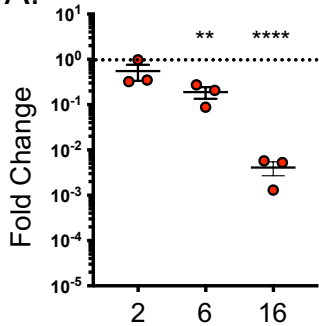
Surface MHC-I



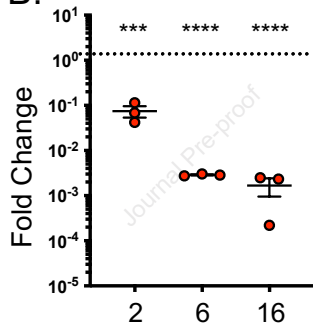
B.



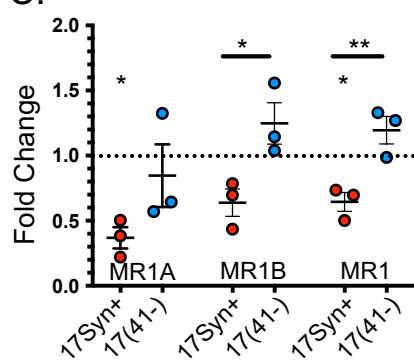
A.

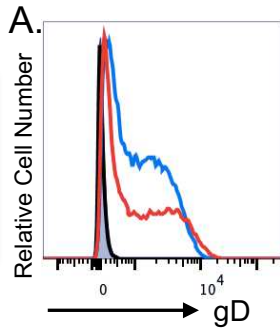


B.

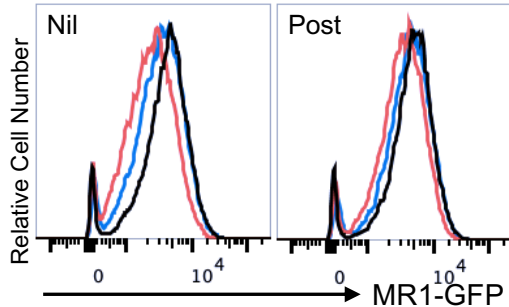
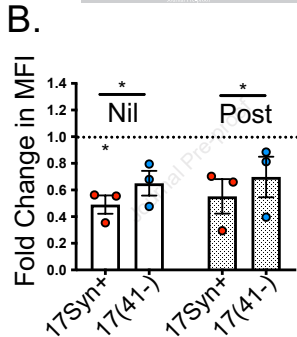


C.

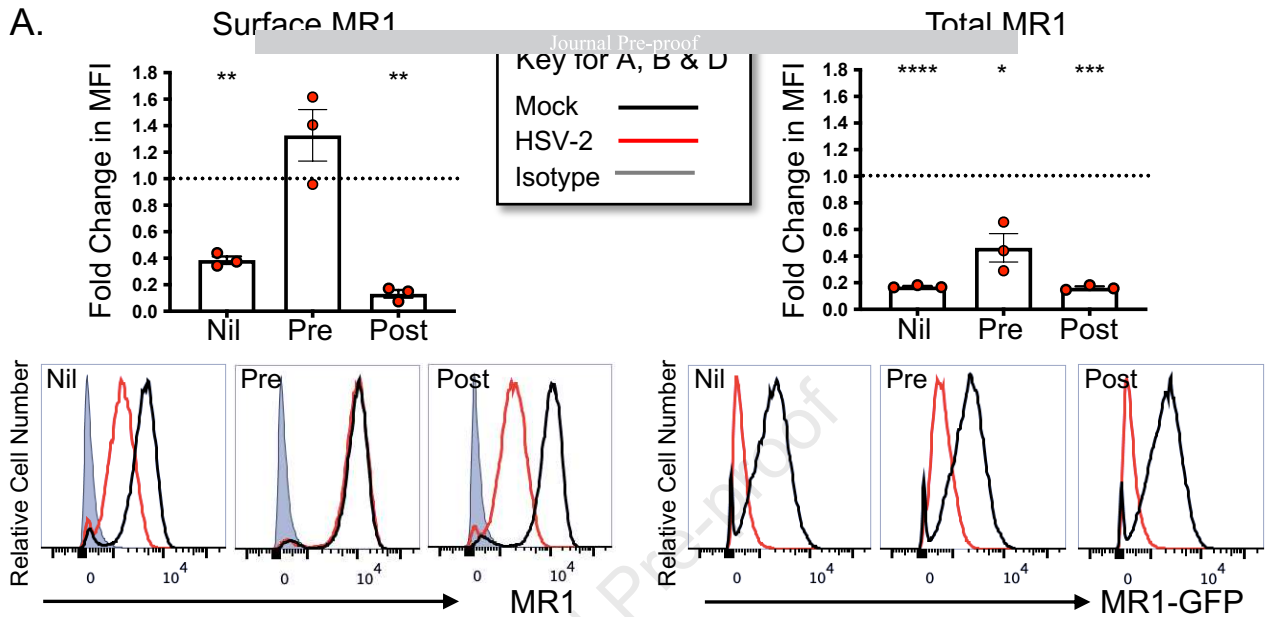




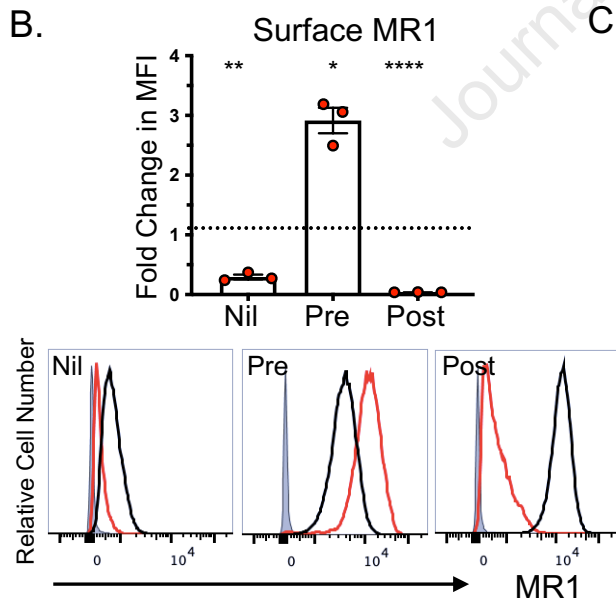
Mock —
 17Syn+ —
 17(41-) —
 Isotype —



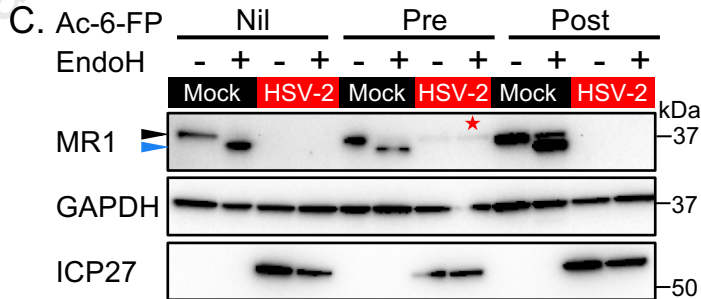
A.



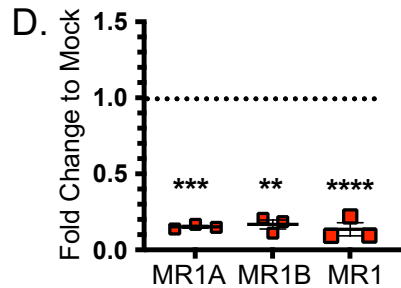
B.



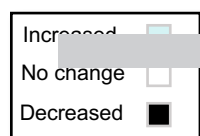
C.



D.

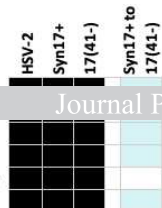


A.



FC to Mock

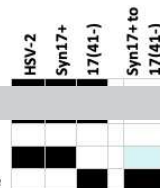
EEA1
LAMP1
Plasma membrane
Cell



B.

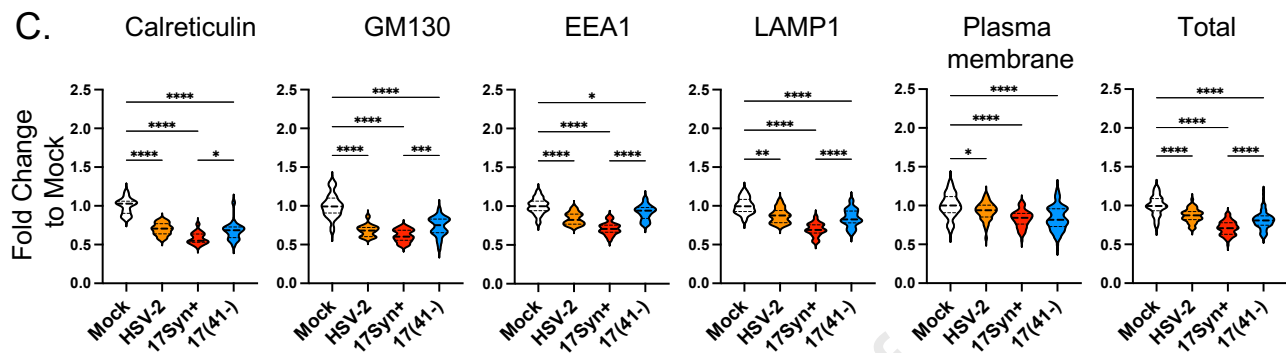
FC to Cell

EEA1
LAMP1
Plasma membrane

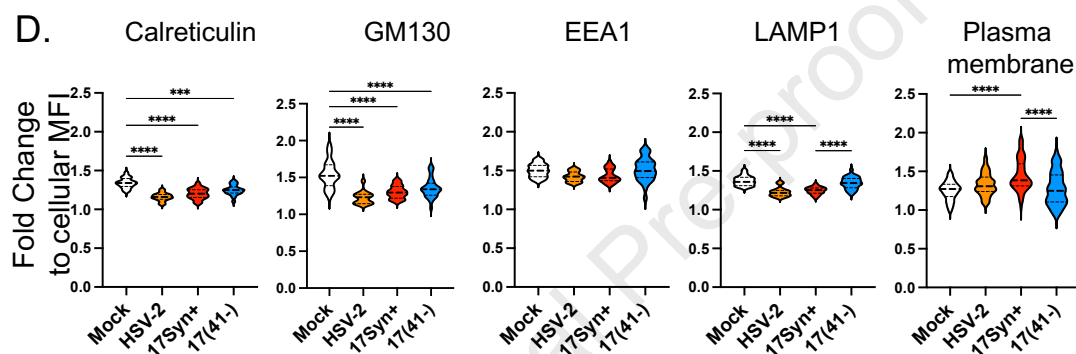


Journal Pre-proof

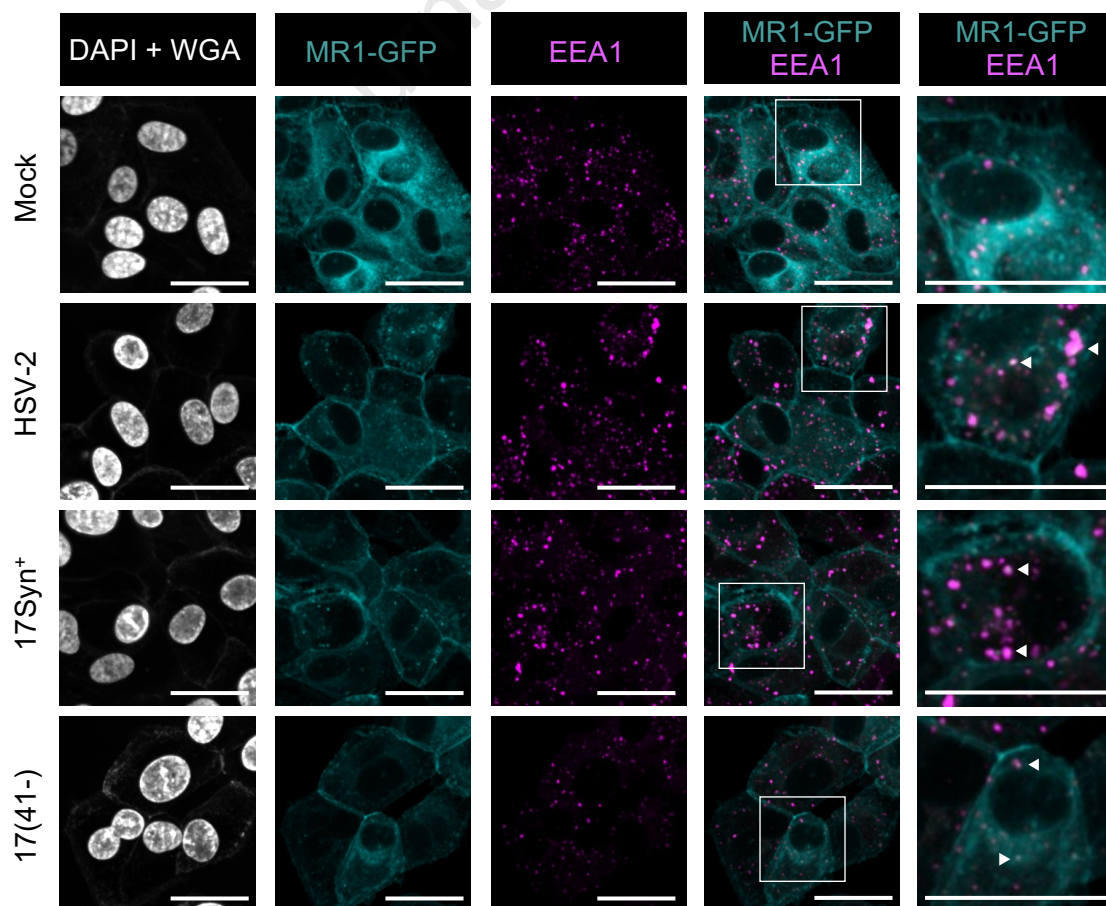
C.



D.



E.



- HSV-1 virion host shutoff (vhs) RNase protein degrades MR1 transcripts
- HSV-1 ICP22 protein targets MR1 for proteasomal degradation
- HSV-2 downregulation of MR1 transcripts and protein mirrors HSV-1 modulation

Journal Pre-proof

KEY RESOURCES TABLE

REAGENT or RESOURCE	SOURCE	IDENTIFIER
Antibodies		
Mouse monoclonal anti-MR1-biotin (clone 26.5)	Jose Villadangos, The Peter Doherty Institute of Infection and Immunity, The University of Melbourne. McWilliam et al., 2016 ⁵¹	N/A
Human recombinant anti-HLA-ABC-PE (clone REA230)	Miltenyi Biotec	Cat#130-120-055; (RRID:AB_2751977)
Mouse monoclonal anti-MR1-PE (clone 26.5)	Biologend	Cat#361105; RRID:AB_2563042
Mouse monoclonal anti-MR1-APC (clone 26.5)	Biologend	Cat#361107; RRID:AB_2563204
Mouse monoclonal anti-HLA-ABC-APC (clone G46-2.6)	BD Biosciences	Cat#555555; RRID:AB_398603
Mouse monoclonal anti-HLA-ABC-SB436 (clone W6/32)	Invitrogen	Cat#62-9983-42; RRID:AB_2688263
Rabbit polyclonal Anti-MR1-CT, generated against the final 15 residues of human MR1 cytosolic tail (PREQNGAIYLPTPDR)	Jose Villadangos, The Peter Doherty Institute of Infection and Immunity, The University of Melbourne. McWilliam et al., 2016 ⁵¹	N/A
Mouse monoclonal anti-MR1	Abcam	Cat#ab55164; RRID:AB_944260
Mouse monoclonal anti-HLA-ABC (clone EMR8-5)	Abcam	Cat#ab70328; RRID:AB_1269092
Mouse monoclonal anti-GFP (clone B-2)	Santa Cruz Biotechnology	Cat#sc-9996; RRID:AB_627695
Rabbit polyclonal anti-GAPDH (FL-335)	Santa Cruz Biotechnology	Cat#sc-25778; RRID:AB_10167668
Rabbit monoclonal anti-DDDDK (clone EPR20018-251)	Abcam	Cat#ab205606; RRID:AB_2916341
Mouse monoclonal anti-HSV-1 ICP27 (clone RAd142)	Santa Cruz Biotechnology	Cat#sc-69806; RRID:AB_1124272
Mouse monoclonal anti-gD-FITC	Virostat	Cat#0196
Mouse monoclonal anti-gC-FITC	Virostat	Cat#0143
Goat polyclonal anti-adenovirus	Sigma-Aldrich	Cat#AB1056; RRID:AB_90213
Live/Dead™ Fixable blue	Invitrogen	Cat#L23105
Zombie NIR™ Fixable Viability Kit	Biologend	Cat#423105
Streptavidin-PE	eBioscience	Cat#12-4317-87
Streptavidin-APC	eBioscience	Cat#17-4317-82
Wheat Germ Agglutinin CF405M conjugate	Biotium	Cat#29028
Rabbit polyclonal anti-calreticulin	Sigma-Aldrich	Cat#C4606; RRID:AB_476843

Rabbit monoclonal anti-GM130 (clone D6B1)	Cell Signaling Technology	Cat#12480; RRID: AB_2797933
Rabbit monoclonal anti-EEA1 (clone F.43.1)	Invitrogen	Cat#MA514794; RRID:AB_10985824
Rabbit polyclonal anti-LAMP1	Abcam	Cat#ab24170; RRID: AB_775978
Donkey anti-Rabbit IgG (H+L) Highly Cross-Adsorbed Secondary Antibody, Alexa Fluor™ 546	Invitrogen	Cat#A10040
DAPI ready made solution	Sigma-Aldrich	Cat#MBD0015
Bacterial and Virus Strains		
HSV-1 Strain F	Dr Russell Diefenbach (Macquarie University)	Accession# GU734771
HSV-1 Strain 17	Prof Roger Everett (University of Glasgow)	Accession# NC_001806
HSV-1 Strain KOS	Dr P Kinchington, Departments of Ophthalmology, and of Molecular Microbiology and Genetics, University of Pittsburgh	Accession# JQ780693
HSV-2 Strain 186	Dr Naomi Truong, The Westmead Institute for Medical Research. Rawls et al., 1968 ¹¹⁴	N/A
HSV-1 Strain 17 vhs mutant 17(41-)	Prof Roger Everett (University of Glasgow). Fenwick and Everett, 1990 ⁷⁹	N/A
HSV-1 Strain KOS US12 mutant ICP47del	Velusamy et al., 2023 ⁴⁸	N/A
SW102 <i>E. coli</i> containing the pAdZ5-C5 vector	Stanton et al., 2008 ⁶⁷	N/A
5-alpha Competent <i>E. coli</i>	NEB	Cat#C2987H
Biological Samples		
Chemicals, Peptides, and Recombinant Proteins		
Dulbecco's Modified Eagle's Medium	Lonza	Cat#12-604F
Hanks Balanced Salt Solution	Gibco	Cat#14170
Fetal Calf Serum	Cytiva	Cat#SH30084.02
Normal donkey serum	Sigma-Aldrich	Cat#D9663
Ac-6-FP Acetyl-6-formylpterin	Schircks	Cat#11.418
BD Cytofix™ Fixation buffer	BD Biosciences	Cat#554655
Folimycin (concanamycin A)	Sigma-Aldrich	Cat#C9705
MG132	Sigma-Aldrich	Cat#M7449
Fugene HD	Promega	Cat#E2231
Q5 High-Fidelity polymerase	NEB	Cat#M0491
Endo H	NEB	Cat#P0703S

DAB Substrate	Pierce	Cat#34065
BamHI-HF	NEB	Cat#R3136
SpeI-HF	NEB	Cat#R3133
BglII	NEB	Cat#R0144
XbaI	NEB	Cat#R0145
Xgal	Abcam	Cat#ab144388
IPTG	Abcam	Cat#ab142072
<i>Hind</i> III	NEB	Cat#R0104
T4 DNA ligase NEB	NEB	Cat#M0202
Geltrex™ basement membrane matrix	Gibco	Cat#A1413301
Critical Commercial Assays		
GFX™ PCR DNA and Gel Band Purification Kit	Cytiva	Cat#28903470
QIAprep Spin Miniprep Kit	QIAGEN	Cat#27106X4
NucleoSpin® Gel and PCR Cleanup	Macherey-Nagel	Cat#740609
NucleoBond® Xtra Midi kit	Macherey-Nagel	Cat#740410
ISOLATE II RNA Mini Kit	Meridian Bioscience	Cat#BIO-52072
Affinity Script cDNA synthesis kit	Aligent Technologies	Cat#600559
Brilliant II SYBR Green qPCR Master Mix	Aligent Technologies	Cat#600828
Deposited Data		
Experimental Models: Cell Lines		
Human fibroblasts HF (male)	ATCC	SCRC-1041; RRID:CVCL_3285
Human ARPE-19 cell line (male)	ATCC	CRL-2302; RRID:CVCL_0145
Human 293T cell line (female)	ATCC	CRL-3216; RRID:CVCL_0063
Human 293A cell line (female)	ATCC	Cat# 305070, RRID:CVCL_6910
Human T-REx™-293 cell line (female)	ThermoFisher	R71007; RRID:CVCL_D585
Green monkey Vero cell line (female)	ATCC	CCL-81; RRID:CVCL_0059
ARPE-19 MR1 (male)	McSharry et al., 2020 ³⁷	N/A
ARPE-19 MR1-GFP (male)	McSharry et al., 2020 ³⁷	N/A
Experimental Models: Organisms/Strains		
Oligonucleotides		
HSV-1 F ICP22 pSY10-ICP22 Forward primer 5'- GTCTACACTAGTATGGCCGACATTTCCCCAGG -3'	This study	N/A
HSV-1 F ICP22 pSY10-ICP22 Reverse primer 5' GTCTACAGATCTCGGCCGAGAAACGTGTGCTG -3'	This study	N/A
See Table S1. Primers used to amplify HSV-1 genes for recombination into pAdZ5-C5 vector	This study	N/A
See Table S2. Primers used for RT-qPCR, Related to STAR methods.	This study	N/A
Recombinant DNA		

pSY10-ICP22	This study	N/A
pCDH_EF1-MCS-T2A-copGFP vector (pSY10)	Systems Bioscience, USA	Cat3#CD526A-1
pAdZ5-C5 (RAd-Ctrl)	Stanton et al., 2008 ⁶⁷	N/A
RAd-ICP22	This study	N/A
RAd-US1.5	This study	N/A
RAd-vhs	This study	N/A
Software and Algorithms		
FlowJo software, Version 10	Treestar Inc.	https://www.flowjo.com/
Paired Student's <i>t</i> tests or ANOVA analysis performed as indicated using Prism software, Version 10	GraphPad	https://www.graphpad.com/scientific-software/prism/
CLC Main Workbench, Version 22	QIAGEN	https://www.qiagenbioinformatics.com/products/clc-main-workbench/
ImageJ FIJI software, Version 1.53t	Schindelin et al., 2012 ¹¹⁶	https://imagej.net/software/fiji/
Ilastik software	Berg et al., 2019 ⁸²	https://www.ilastik.org/
Other		